

Structural risk minimization for quantum linear classifiers

Casper Gyurik ¹^{*1}, Dyon van Vreumingen ^{†1,2,3}, and Vedran Dunjko ^{‡1}

¹Leiden University, Niels Bohrweg 1, 2333 CA Leiden, the Netherlands

²QuSoft, Science Park 123, 1098 XG Amsterdam, the Netherlands

³Institute of Physics, University of Amsterdam, Science Park 904, 1098 XH Amsterdam, the Netherlands

May 13, 2021

Abstract

Quantum machine learning (QML) stands out as one of the typically highlighted candidates for quantum computing’s near-term “killer application”. In this context, QML models based on parameterized quantum circuits comprise a family of machine learning models that are well suited for implementations on near-term devices and that can potentially harness computational powers beyond what is efficiently achievable on a classical computer. However, how to best use these models – e.g., how to control their expressivity to best balance between training accuracy and generalization performance – is far from understood. In this paper we investigate capacity measures of two closely related QML models called explicit and implicit quantum linear classifiers (also called the quantum variational method and quantum kernel estimator) with the objective of identifying new ways to implement structural risk minimization – i.e., how to balance between training accuracy and generalization performance. In particular, we identify that the rank and Frobenius norm of the observables used in the QML model closely control the model’s capacity. Additionally, we theoretically investigate the effect that these model parameters have on the training accuracy of the QML model. Specifically, we show that there exists datasets that require a high-rank observable for correct classification, and that there exists datasets that can only be classified with a given margin using an observable of at least a certain Frobenius norm. Our results provide new options for performing structural risk minimization for QML models.

1 Introduction

After years of efforts the first proof-of-principle quantum computations that surpass what is feasible with classical supercomputers have been realized [1]. As the leap from noisy intermediate-scale quantum (NISQ) devices [2] to full-blown quantum computers may require further decades, finding practically useful NISQ-suitable algorithms is becoming increasingly important. It has been argued that some of the most promising NISQ-suitable algorithms are those that rely on *parameterized quantum circuits* (also called variational quantum circuits) [3, 4]. Such algorithms have been proposed for quantum chemistry [5, 6, 7], for optimization [8], and for machine learning [9]. One

^{*}c.f.s.gyurik@liacs.leidenuniv.nl

[†]dyon.van.vreumingen@cwi.nl

[‡]v.dunjko@liacs.leidenuniv.nl

of the advantages of parameterized quantum circuits is that restrictions of NISQ devices can be hardwired into the circuit. Moreover, families of parameterized quantum circuits can – under widely believed complexity-theoretic assumptions – realize input-output correlations that are intractable for classical computation [10, 11]. In this paper we discuss the application of parameterized quantum circuits as machine learning models in hybrid quantum-classical methods. The use of NISQ devices in the context of machine learning is particularly appealing as machine learning algorithms may be more tolerant to noise in the quantum hardware [12, 13]. In short, parameterized quantum circuits offer the tantalizing possibility of machine learning models that cannot be efficiently evaluated on a classical computer, that could conceivably be used to learn complex data for which conventional models may struggle, while being well-suited for implementations on NISQ devices.

In machine learning, parameterized quantum circuits can serve as a parameterized family of real-valued functions in a manner similar to neural networks (they are also often called quantum neural networks). It has been noted that machine learning models based on parameterized quantum circuit are closely related to so-called *linear classifiers*, which use hyperplanes to separate classes of data embedded in a vector space. This connection was first established by Havlíček et al. [14], and Schuld & Killoran [15], who both defined two machine learning models based on parameterized quantum circuits that efficiently implement certain families of linear classifiers – an illustration of which can be found in Figure 1. In this paper we further investigate and exploit this relation between machine learning models based on parameterized quantum circuits and standard linear classifiers in order to investigate how to perform *structural risk minimization*. More specifically, we study how to tune certain parameters of the quantum machine learning model in order to optimize its expressivity (i.e., the ability to capture correlations in the training examples) while preventing the model from becoming too complex (which could cause it to overfit and generalize poorly).

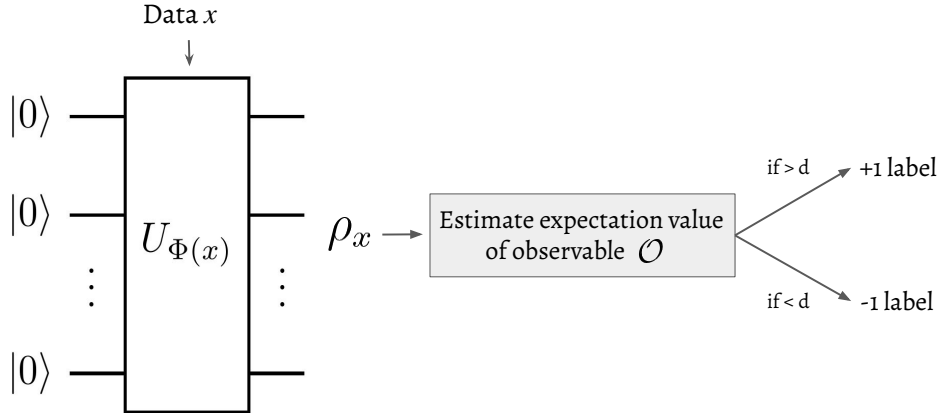


Figure 1: An overview of the quantum machine learning models introduced in [14, 15]. First, a parameterized quantum circuit is used to encode the data into a quantum state ρ_x . Afterwards, an observable \mathcal{O} is measured. If its expectation value lies above d , then we assign the label $+1$, and -1 otherwise. The goal in training is the find the optimal observable \mathcal{O} and threshold d .

Main contributions We investigate which model parameters can be used to implement structural risk minimization for a family of quantum machine learning models that includes the models introduced by Havlíček et al. [14], and Schuld & Killoran [15]. Specifically, we theoretically analyze

the effect that limiting the rank or Frobenius norm of the observables measured by these models has on the trade-off between 1. generalization performance, and 2. expressivity, and we show that:

1. (a) A measure of capacity called the *VC dimension* can be controlled by limiting the *rank* of the observables measured by the quantum model. In particular, we provide explicit analytical bounds on the VC dimension in terms of the rank of the observable.
- (b) A measure of capacity called the *fat-shattering dimension* can be controlled by limiting the *Frobenius norm* of the observables measured by the quantum model. In particular, we provide explicit analytical bounds on the fat-shattering dimension in terms of the Frobenius norm of the observable.

Due to the well established connection between these capacity measures and generalization performances [16, 17], our results theoretically quantify the effect that adjusting these model parameters has on the generalization performance of the quantum model.

2. (a) Quantum models that use high-rank observables are strictly more expressive than quantum models that use low-rank observables. In particular, we show that i) any set of examples that can be correctly classified using a low-rank observable can also be correctly classified using a high-rank observable, and ii) that there exist sets of examples that can only be correctly classified using an observable of at least a certain rank.
- (b) Quantum models that use observables with large Frobenius norms can achieve larger margins – i.e., empirical quantities that can be measured when training on a set of examples and which influence certain generalization bounds – compared to quantum models that use observables with small Frobenius norms. In particular, we show that there exist sets of examples that can only be correctly classified with a given margin using observables of at least a certain Frobenius norm. Since the Frobenius norm controls the fat-shattering dimension, this can actually also have a positive effect on the generalization performance (as discussed in Section 3.1).

To summarize, we show that increasing the rank or Frobenius norm of the observables measured by the quantum machine model increases the over expressivity of the model.

Additional to the above two points, we also connect to standard structural risk minimization theory and discuss how to use our results to find the best quantum models in practice. In particular, we discuss different types of regularization that are theoretically motivated by our results. Moreover, we find that there exist training methods – i.e., those who penalize high-rank observables – that are meaningful and for which the relationship between the two quantum models [18] does not apply.

Related work Other work in this direction has focused on showing that these quantum models are remarkably expressive [19] and satisfy generalization bounds based on other capacity measures [20]. There has also been work on determining capacity measures of these quantum models and showing how they depend on the parameterized quantum circuit ansatz [21, 22, 23] or the level of noise [24]. Finally, there has been work that studied the generalization performance of quantum models in order to investigate whether they can perform better than classical models [25, 26, 27].

Organization In Section 2, we define the quantum machine learning models studied in this paper. In Section 3, we investigate how structural risk minimization can be achieved for these quantum

models. Firstly, in Subsection 3.1, we recap some background on structural risk minimization. We then determine two capacity measures of the quantum models allowing us to identify model parameters that control the models complexity in Subsection 3.2. Afterwards, we investigate the effect of these model parameters on the empirical performance in Subsection 3.3. We end the paper with a discussion of how to use our results to implement structural risk minimization of the quantum models in practice in Subsection 3.4. All proofs are deferred to the appendix.

2 Quantum linear classifiers: implicit and explicit approaches

A fundamental family of classifiers used throughout machine learning are those based on so-called *linear functions*. Specifically, they are based on the family of real-valued functions on \mathbb{R}^ℓ given by

$$\mathcal{F}_{\text{lin}} = \left\{ f_w(x) = \langle w, x \rangle \mid w \in \mathbb{R}^\ell \right\}, \quad (1)$$

where $\langle \cdot, \cdot \rangle$ denotes an inner product on the input space \mathbb{R}^ℓ . These linear functions are turned into classifiers by adding an offset and considering the sign, i.e., the classifiers are given by

$$\mathcal{C}_{\text{lin}} = \left\{ c_{w,d}(x) = \text{sign}(\langle w, x \rangle - d) \mid w \in \mathbb{R}^\ell, d \in \mathbb{R} \right\}. \quad (2)$$

These linear classifiers essentially use hyperplanes to separate the different classes in the data.

While this family of classifiers seems relatively limited, it becomes powerful when introducing a so-called *feature map*. Specifically, a feature map $\Phi : \mathbb{R}^\ell \rightarrow \mathbb{R}^N$ is used to (non-linearly) map the data to a (much) higher-dimensional space – called the *feature space* – in order to make the data more linearly-separable. We let $\mathcal{C}(\Phi) = \{c \circ \Phi \mid c \in \mathcal{C}\}$ denote the family of classifiers on \mathbb{R}^ℓ obtained by combining a family of linear classifiers $\mathcal{C} \subseteq \mathcal{C}_{\text{lin}}$ on \mathbb{R}^N with a feature map Φ . If the feature map is clear from the context we will omit it in the notation and just write \mathcal{C} . A well known example of a model based on linear classifiers is the so-called *support vector machine* (SVM), which aims to finds the hyperplane that attains the maximal perpendicular distance to the two classes of points in the two distinct half-spaces (assuming the feature map makes the data linearly-separable).

The linear-algebraic nature of linear classifiers makes them particularly well-suited for quantum treatment. In the influential works of Havlíček et al. [14], and Schuld & Killoran [15], the authors propose a model where the space of n -qubit Hermitian operators – denoted by $\text{Herm}(\mathbb{C}^{2^n})$ – takes the role of the feature space. Specifically, they consider $\text{Herm}(\mathbb{C}^{2^n})$ as a 4^n -dimensional real vector space equipped with the Frobenius inner product $\langle A, B \rangle = \text{Tr}[A^\dagger B]$. Their feature map – which we refer to as a *quantum feature map* – maps inputs $x \mapsto \rho_x$, where ρ_x is an n -qubit density matrix. Finally, the hyperplanes used to separate the states ρ_x corresponding to different classes are n -qubit observables. That is, the family of linear functions their model uses is given by

$$\mathcal{F}_{\text{qlin}} = \left\{ f_{\mathcal{O}}(\rho_x) = \text{Tr}[\mathcal{O}\rho_x] \mid \mathcal{O} \in \text{Herm}(\mathbb{C}^{2^n}) \right\}, \quad (3)$$

and the family of classifiers – which we refer to as *quantum linear classifiers* – is given by

$$\mathcal{C}_{\text{qlin}} = \left\{ c_{\mathcal{O},d}(x) = \text{sign}(\text{Tr}[\mathcal{O}\rho_x] - d) \mid \mathcal{O} \in \text{Herm}(\mathbb{C}^{2^n}), d \in \mathbb{R} \right\}. \quad (4)$$

We can estimate $f_{\mathcal{O}}(\rho_x)$ defined in Equation (3) by preparing the state ρ_x and measuring the observable \mathcal{O} . Using parameterized quantum circuits both of this can be done efficiently for certain

families of feature maps and observables. We now briefly recap two ways in which parameterized quantum circuits can be used to efficiently implement a family of quantum linear classifiers, as originally proposed by Havlíček et al. [14], and Schuld & Killoran [15]. Both ways use a parameterized quantum circuit to implement the feature map. Specifically, let U_Φ be a parameterized quantum circuit, then we can use it to construct the feature map given by

$$\Phi : x \mapsto \rho_\Phi(x) := |\Phi(x)\rangle \langle \Phi(x)|, \quad (5)$$

where $|\Phi(x)\rangle := U_\Phi(x) |0\rangle^{\otimes n}$. The key difference between the two approaches is which observables they are able to implement (i.e., which separating hyperplanes they can represent) and how the observables are actually measured (i.e., how the functions $f_{\mathcal{O}}$ are evaluated). An overview of how the two approaches implement quantum linear classifiers can be found in Figure 2, and we discuss the main ideas behind the two approaches below.

Explicit quantum linear classifier¹ The observables measured in this approach are implemented by first applying a parameterized quantum circuit $W(\theta)$, followed by a computational basis measurement and possible postprocessing of the outcome $\lambda : [2^n] \rightarrow \mathbb{R}$. In short, the corresponding observable is given by

$$\mathcal{O}_\theta = W^\dagger(\theta) \cdot \text{diag}(\lambda(0), \lambda(1), \dots, \lambda(2^n - 1)) \cdot W(\theta). \quad (6)$$

Examples of efficiently computable postprocessing functions λ include functions with a polynomially small support (implemented using a lookup table), functions that are efficiently computable from the input bitstring (e.g., the parity of the bitstring, which is equivalent to measuring $Z^{\otimes n}$), or parameterized functions such as neural networks. Altogether, this efficiently implements the family of linear classifiers – which we refer to as *explicit quantum linear classifiers* – given by

$$\mathcal{C}_{\text{qlin}}^{\text{explicit}} = \left\{ c_{\mathcal{O}_\theta, d}(x) = \text{sign}(\text{Tr}[\rho_\Phi(x)\mathcal{O}_\theta] - d) \mid \mathcal{O}_\theta \text{ as in Equation (6), } d \in \mathbb{R} \right\}. \quad (7)$$

The power of this model lies in the efficient parameterization of the manifold (inside the 4^n -dimensional vector space of Hermitian operators on \mathbb{C}^{2^n}) realized by the quantum feature map together with the parameterized hyperplanes that can be attained by $W(\theta)$. Here also lies a restriction of the explicit quantum linear classifier compared to standard linear classifiers, as in the latter all hyperplanes are possible and in the former only the hyperplanes that lie in the manifold parameterized by $W(\theta)$ and λ are possible. Note that it requires a number of parameters that is exponential in the number of qubits in order to parameterize all possible separating hyperplanes (i.e., the entire space of n -qubit observables) due to the exponential dimension of $\text{Herm}(\mathbb{C}^{2^n})$. Furthermore, explicit quantum linear classifiers can likely not be efficiently evaluated classically, as computing expectation values $\text{Tr}[\rho_\Phi(x)\mathcal{O}_\theta]$ is classically intractable for sufficiently complex feature maps and observables [10, 11].

Implicit quantum linear classifier² Another way to implement a linear classifier is by using the so-called *kernel trick*. In short, this trick involves expressing the normal vector of the separating

¹Also called the *quantum variational classifier* [14].

²Also called the *quantum kernel estimator* [14].

hyperplane w on a set of training examples \mathcal{D} as a linear combination of feature vectors, resulting in the expression

$$w = \sum_{x' \in \mathcal{D}} \alpha_{x'} \Phi(x').$$

Using this expression we can rewrite the corresponding linear classifier as

$$c_{w,d}(x) = \text{sign}(\langle w, \Phi(x) \rangle - d) = \text{sign}\left(\sum_{x' \in \mathcal{D}} \alpha_{x'} \langle \Phi(x'), \Phi(x) \rangle - d\right).$$

These type of linear classifiers can also be efficiently realized using parameterized quantum circuits. Using quantum protocols such as the SWAP-test or the Hadamard-test it is possible to efficiently evaluate the overlaps $\text{Tr}[\rho_\Phi(x)\rho_\Phi(x')]$ for the feature map defined in Equation (5). Afterwards, the optimal parameters $\{\alpha_{x'}\}_{x' \in \mathcal{D}}$ are obtained, e.g., by solving a quadratic program on a classical computer. Altogether, this allows us to efficiently implement the family of linear classifiers – which we refer to as *implicit quantum linear classifiers* – given by

$$\mathcal{C}_{\text{qlin}}^{\text{implicit}} = \left\{ c_{\mathcal{O}_\alpha, d}(x) = \text{sign}(\text{Tr}\rho_\Phi(x)\mathcal{O}_\alpha - d) \mid \mathcal{O}_\alpha = \sum_{x' \in \mathcal{D}} \alpha_{x'} \rho_\Phi(x), \alpha \in \mathbb{R}^{|\mathcal{D}|}, d \in \mathbb{R} \right\}. \quad (8)$$

The power of this model comes from the fact that evaluating the overlaps $\text{Tr}[\rho_\Phi(x)\rho_\Phi(x')]$ is likely classically intractable for sufficiently complex feature maps [14], demonstrating that classical computers can likely neither train nor evaluate this quantum linear classifier efficiently.

As we will discuss in more detail in Section 3.4, any quantum linear classifier that minimizes a cost functions which includes so-called *regularization* of the Frobenius norm of the observable can be expressed as an implicit quantum linear classifier [18]. However, as we indicate later in Section 3.4, this does not mean that we can forego explicit quantum linear classifiers, as in the explicit picture there are unique types of meaningful regularization that have no straightforward equivalent in the implicit picture. Moreover, for these types of regularization there are no theoretical guarantees on the structure and performance of the minimizing classifiers.

3 Structural risk minimization for quantum linear classifiers

When looking for the optimal family of classifiers for a given learning problem, it is important to carefully select the family's so-called complexity (also known as expressivity or capacity). For instance, in the case of linear classifiers, it is important to select what kind of hyperplanes you allow your classifiers to use. In general, the more complex the family is, the lower the training errors will be. However, if the family becomes overly complex, then it is prone to worse generalization performance (e.g., due to overfitting). Structural risk minimization is a concrete method that balances this trade-off to minimize the expected error to obtain the best possible performance on unseen examples. Specifically, structural risk minimization aims to saturate an upper bound on the expected error that consists of the sum of two inversely related terms – i.e., a *training error* and a *complexity term* that penalizes more complex models.

In this section we carefully analyze and quantify the influence that certain hyperparameters of quantum linear classifiers have in the framework of structural risk minimization. First, we discuss some of the background of structural risk minimization and introduce the expected error bound on which it relies. Afterwards, we analyse the complexity term in the expected error bound and

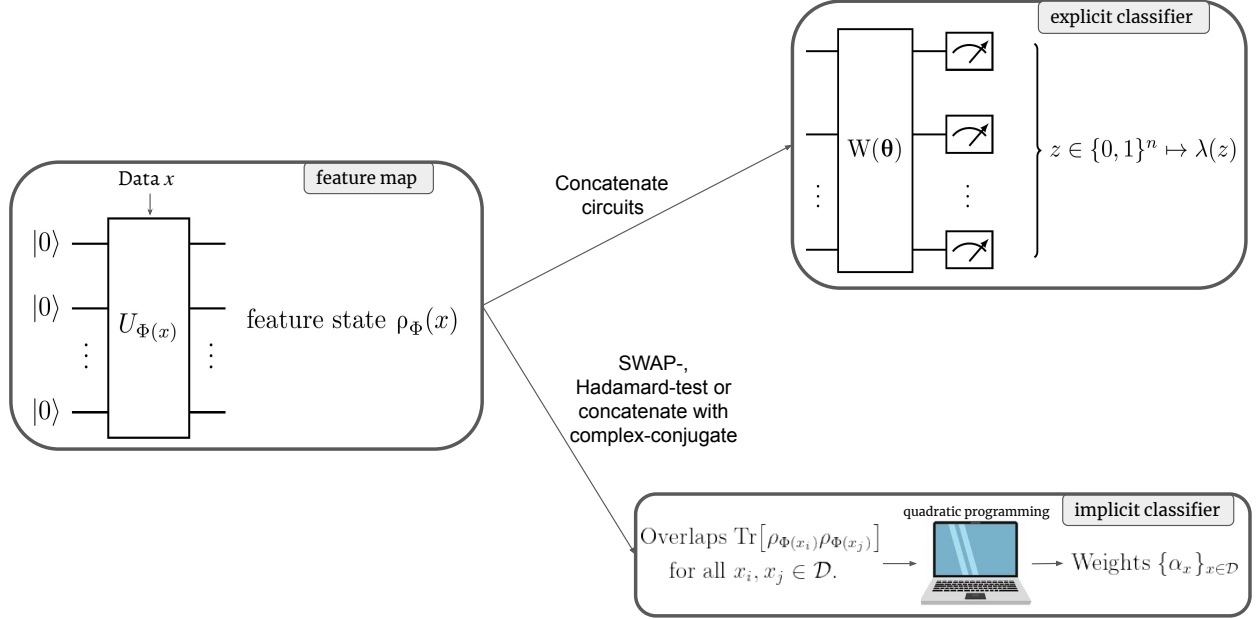


Figure 2: An overview of the implementations of the explicit and implicit quantum linear classifiers defined in Equations (7) and (8), respectively. Note that in the case of the explicit classifier, a universal circuit $W(\theta)$ (producing the eigenbasis) followed by a computational basis measurement and universal postprocessing λ (producing the eigenvalues) allows one to measure any observable.

identify model parameters that allow us to control it. Based on this analysis we study the influence that these model parameters have on the training error term in the expected error bound. Finally, we discuss how to implement structural risk minimization of quantum linear classifiers in practice based on the results obtained in this section.

3.1 Background

In machine learning it is generally assumed that the data is sampled according to some underlying probability distribution P on $\mathcal{X} \times \{-1, +1\}$. The goal is to find a classifier that minimizes the probability that a random pair sampled according to P is misclassified. That is, the goal is to find a classifier $c_{f,d}(x) = \text{sign}(f(x) - d)$ that minimizes the *expected error* given by

$$\text{er}_P(c_{f,d}) = \Pr_{(x,y) \sim P}(c_{f,d}(x) \neq y). \quad (9)$$

As one generally only has access to training examples $\mathcal{D} = \{(x_1, y_1), \dots, (x_m, y_m)\}$ that are sampled according to the distribution P , it is not possible to compute er_P directly. Nonetheless, one can try to approximate Equation (9) using *training errors* such as

$$\hat{\text{er}}_{\mathcal{D}}(c_{f,d}) = \frac{1}{m} \left| \{i \mid c_{f,d}(x_i) \neq y_i\} \right|, \quad (10)$$

$$\hat{\text{er}}_{\mathcal{D}}^{\gamma}(c_{f,d}) = \frac{1}{m} \left| \{i \mid y_i \cdot (f(x_i) - d) < \gamma\} \right|, \quad \gamma \in \mathbb{R}_{\geq 0}. \quad (11)$$

Intuitively, $\widehat{er}_{\mathcal{D}}$ in Equation (10) represents the number of misclassified training examples, and $\widehat{er}_{\mathcal{D}}^{\gamma}$ in Equation (11) represents the number of training examples that are either misclassified or are “within margin γ from being misclassified”. In particular, for $\gamma = 0$ both training error estimates are identical (i.e., $\widehat{er}_{\mathcal{D}} = \widehat{er}_{\mathcal{D}}^0$). When talking about the expressivity of a family of classifiers, we generally refer to its ability to achieve small training errors on varying sets of training examples.

Structural risk minimization uses expected error bounds – two of which we will discuss shortly – that involve a training error term and a complexity term that penalizes more complex models. This complexity term usually scales with a certain measure of the capacity of the family of classifiers. A well known example of such a capacity measure is the Vapnik-Chervonenkis dimension.

Definition 1 (VC dimension [28]). *Let \mathcal{C} be a family of functions on \mathcal{X} taking values in $\{-1, +1\}$. We say that a set of points $X = \{x_1, \dots, x_m\} \subset \mathcal{X}$ is shattered by \mathcal{C} if for all $y \in \{-1, +1\}^m$, there exists a classifier $c_y \in \mathcal{C}$ that satisfies $c_y(x_i) = y_i$. The VC dimension of \mathcal{C} defined as*

$$\text{VC}(\mathcal{C}) = \max \{m \mid \exists \{x_1, \dots, x_m\} \subset \mathcal{X} \text{ that is shattered by } \mathcal{C}\}.$$

Besides the VC dimension we also consider another capacity measure called the *fat-shattering dimension*, which can be viewed as a generalization of the VC dimension to real-valued functions. An important difference between the VC dimension and the fat-shattering dimension is that the latter also takes into account the so-called *margins* that the family of classifiers can achieve. Here the margin of a classifier $c_{f,d}(x) = \text{sign}(f(x) - d)$ on a set of examples $\{x_i\}_{i=1}^m$ is given by $\max_i |f(x_i) - d|$.

Definition 2 (Fat-shattering dimension [29]). *Let \mathcal{F} be a family of real-valued functions on \mathcal{X} . We say that a set of points $X = \{x_1, \dots, x_m\} \subset \mathcal{X}$ is γ -shattered by \mathcal{F} if there exists an $s \in \mathbb{R}^m$ such that for all $y \in \{-1, +1\}^m$, there is a function $f_y \in \mathcal{F}$ satisfying*

$$f_y(x_i) \begin{cases} \leq s_i - \gamma & \text{if } y_i = -1, \\ \geq s_i + \gamma & \text{if } y_i = +1. \end{cases}$$

The fat-shattering dimension of \mathcal{F} is a function $\text{fat}_{\mathcal{F}} : \mathbb{R} \rightarrow \mathbb{Z}_{\geq 0}$ that maps

$$\text{fat}_{\mathcal{F}}(\gamma) = \max \{m \mid \exists \{x_1, \dots, x_m\} \subset \mathcal{X} \text{ that is } \gamma\text{-shattered by } \mathcal{F}\}.$$

Remark(s). For linear classifiers the γ is related to the margin of the separating hyperplane, i.e., the margin of a separating hyperplane with normal vector w is equal to $\gamma/\|w\|^2$.

The expected error bounds that are used to perform structural risk minimization are stated in the following two theorem. These theorems quantify how an increase in model capacity (i.e., VC dimension or fat-shattering dimension) results in a worse expected error (e.g., due to overfitting). First, we state the expected error bound that involves the VC dimension.

Theorem 1 (Expected error bound using VC dimension [16]). *Consider a set of functions \mathcal{C} on \mathcal{X} taking values in $\{-1, +1\}$. Suppose $\mathcal{D} = \{(x_1, y_1), \dots, (x_m, y_m)\}$ is sampled using m independent draws from P . Then, with probability at least $1 - \delta$, the following holds for all $c \in \mathcal{C}$:*

$$\text{er}_P(c) \leq \widehat{er}_{\mathcal{D}}(c) + \sqrt{\frac{8}{m} \left(k \log(2em/k) + \log(4/\delta) \right)}. \quad (12)$$

where $k = \text{VC}(\mathcal{C})$.

Next, we state the expected error bound that involves the fat-shattering dimension. One possible advantage of using the fat-shattering dimension instead of the VC dimension is that it can take into account the margin that your classifier achieves on the training examples. This turns out to be useful since this margin can be used to more precisely fine-tune the expected error bound.

Theorem 2 (Expected error bound using fat-shattering dimension [17]). *Consider a set of real-valued functions \mathcal{F} on \mathcal{X} . Suppose $\mathcal{D} = \{(x_1, y_1), \dots, (x_m, y_m)\}$ is sampled using m independent draws from P . Then, with probability at least $1 - \delta$, the following holds for all $c(x) = \text{sign}(f(x) - d)$ with $f \in \mathcal{F}$ and $d \in \mathbb{R}$:*

$$\text{er}_P(c) \leq \hat{\text{er}}_{\mathcal{D}}^{\gamma}(c) + \sqrt{\frac{2}{m} \left(k \log(34em/k) \log_2(578m) + \log(4/\delta) \right)}. \quad (13)$$

where $k = \text{fat}_{\mathcal{F}}(\gamma/16)$ and $\gamma = \min_i |f(x_i) - d|$.

Generally, the more complex a family of classifiers is, the larger its generalization errors will be. This correlation between a family's complexity and its generalization errors is clearly illustrated in Theorem 1. Specifically, the more complex the family is the larger its VC dimension will be, which strictly increases the second term in Equation 12 that corresponds to the generalization error. However, for the fat-shattering dimension in Theorem 2 this is not the case, at least not trivially. In particular, a more complex model could achieve a larger margin γ , which actually decreases the second term in Equation 13 that corresponds to the generalization error.

Theorems 1 and 2 establish that in order to minimize the expected error, we should aim to minimize either of the sums on the right-hand side of Equations (12) or (13) (depending on which capacity measure you wish to focus). Note that in both cases the first term corresponds to a training error and the second term corresponds to a complexity term that penalizes more complex models. Crucially, the effect that the capacity measure of the family of classifiers has on these terms is inversely related. Namely, a large capacity measure generally gives rise to smaller training errors, but at the cost of a larger complexity term. Balancing this trade-off is precisely the idea behind structural risk minimization. More precisely, structural risk minimization selects a classifier that minimizes either of the expected error bounds stated in Theorem 1 or 2, by selecting the classifier from a family whose capacity measure is fine-tuned in order to balance both terms on the right-hand side of Equations (12) and (13). Note that limiting the VC dimension and fat-shattering dimension does not achieve the same theoretical guarantees on the generalization error, and it will generally give rise to different performances in practice (as also discussed Section 3.3). An overview of the trade-off happening in the error bounds stated in Theorems 1 and 2 is depicted in Figure 3.

3.2 Capacity of quantum linear classifiers: fat-shattering and VC dimension

In this section we determine the two capacity measures defined in the previous section – i.e., the fat-shattering dimension and VC dimension – for families of quantum linear classifiers. As a result, we identify model parameters that allow us to control the complexity term in the expected error bounds of Theorems 1 and 2. In particular, these model parameters can therefore be used to balance the trade-off considered by structural risk minimization, as depicted in Figure 3.

Throughout this section we fix the feature map to be the one defined Equation (5), we consider a family of observables $\mathbb{O} \subseteq \text{Herm}(\mathbb{C}^{2^n})$ – e.g., the family of observables implementable using either the explicit or implicit realization of quantum linear classifiers – and we determine the capacity

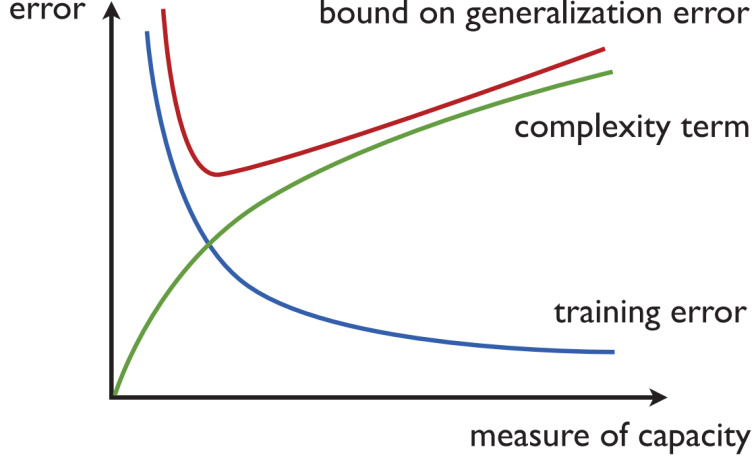


Figure 3: Illustration of structural risk minimization taken from [16]. Increasing the capacity of the classifier family causes the training error (blue) to decrease, while it increases the complexity term (green). Structural risk minimization selects the classifier minimizing the expected error bound in Equations (12) and (13) given by the sum of the training error and the complexity term (red).

measures of the corresponding family of classifiers. First, we show that the VC dimension of a family of quantum linear classifiers depends on the ranks of the observables that it uses. In particular, we show that we can control the VC dimension of a family of quantum linear classifiers by limiting the ranks of its observables. We defer the proof to Appendix A.1.

Proposition 3. *Let $\mathbb{O} \subseteq \text{Herm}(\mathbb{C}^{2^n})$ be a family of n -qubit observables with $r = \dim(\sum_{\mathcal{O} \in \mathbb{O}} \text{Im } \mathcal{O})$ ³. Then, the VC dimension of*

$$\mathcal{C}_{\text{qlin}}^{\mathbb{O}} = \left\{ c(\rho) = \text{sign}(\text{Tr}[\mathcal{O}\rho] - d) \mid \mathcal{O} \in \mathbb{O}, d \in \mathbb{R} \right\} \quad (14)$$

is upper bounded by

$$\text{VC}(\mathcal{C}_{\text{qlin}}^{\mathbb{O}}) \leq r + 1. \quad (15)$$

Remark(s). The quantity r in the above proposition is indeed related to the rank of the observables. For example, note that for any two observables $\mathcal{O}, \mathcal{O}' \in \text{Herm}(\mathbb{C}^{2^n})$ we have that

$$\dim(\text{Im } \mathcal{O} + \text{Im } \mathcal{O}') = \text{rank}(\mathcal{O}) + \text{rank}(\mathcal{O}') - \dim(\text{Im } \mathcal{O} \cap \text{Im } \mathcal{O}').$$

The above proposition shows that the VC dimension of a family of explicit quantum linear classifiers is upper bounded by dimension of the span of the columns of the unitaries $W(\theta)$ corresponding to the nonzero eigenvalues of the observable measured after the parameterized quantum circuit. Moreover, the above proposition also shows that the VC dimension of a family of implicit quantum linear classifiers is upper bounded by the number of training examples. To see this, note that each ρ_x is of rank 1, and thus that $\{\rho_x\}_{x \in \mathcal{D}}$ spans a subspace of dimension at most $|\mathcal{D}|$.

Next, we show that the fat-shattering dimension of a family of quantum linear classifiers is related to the Frobenius norm of the observables that it uses. In particular, we show that we

³Here \sum denotes the sum of vector spaces.

can control the fat-shattering dimension of a family of quantum linear classifiers by limiting the Frobenius norm of its observables. We defer the proof to Appendix A.2, where we also discuss the implications of this result in the probably approximately correct (PAC) learning framework.

Proposition 4. *Let $\mathbb{O} \subseteq \text{Herm}(\mathbb{C}^{2^n})$ be a family of n -qubit observables with $\eta = \max_{\mathcal{O} \in \mathbb{O}} \|\mathcal{O}\|_F$. Then, the fat-shattering dimension of*

$$\mathcal{F}_{\text{qlin}}^{\mathbb{O}} = \left\{ f_{\mathcal{O}, d}(\rho) = \text{Tr}[\mathcal{O}\rho] - d \mid \mathcal{O} \in \mathbb{O}, d \in \mathbb{R} \right\} \quad (16)$$

is upper bounded by

$$\text{fat}_{\mathcal{F}_{\text{qlin}}^{\mathbb{O}}}(\gamma) \leq O\left(\frac{\eta^2}{\gamma^2}\right). \quad (17)$$

Remark(s). The upper bound in the above proposition matches the result discussed in [27]. This was derived independently by one of the authors of this paper [30], and we include it here for completeness.

3.3 Expressivity quantum linear classifiers: model parameters & training errors

In this section we investigate the influence that the model parameters identified in the previous section (i.e., the rank and Frobenius norm of the observables) have on the training errors that the classifiers can achieve. First, we study the influence of these model parameters on the ability of the classifiers to correctly classify certain sets of examples. Afterwards, we study the influence of these model parameters on the margins that the classifiers can achieve.

Recall from the previous section that the VC dimension of a family of quantum linear classifiers depends on the ranks of the observables that it uses. Since the VC dimension is only concerned with whether an example is correctly classified (and not what margin it achieves), we choose to investigate the influence of the rank on being able to correctly classify certain sets of examples. In particular, we show that any set of examples that can be classified using a low-rank observable without having examples on the separating hyperplane, can also be correctly classified using a high-rank observable. Moreover, we also show that there exist sets of examples that can only be correctly classified using observables of at least a certain rank. We defer the proof to Appendix B.1.

Proposition 5. *Let $\mathcal{C}_{\text{qlin}}^{(r)}$ denote the family of quantum linear classifiers corresponding to observables of rank r , that is,*

$$\mathcal{C}_{\text{qlin}}^{(r)} = \left\{ c(\rho) = \text{sign}(\text{Tr}[\mathcal{O}\rho] - d) \mid \mathcal{O} \in \text{Herm}(\mathbb{C}^{2^n}), \text{rank}(\mathcal{O}) = r, d \in \mathbb{R} \right\} \quad (18)$$

Then, the following statements hold:

- (i) *For every finite set of examples \mathcal{D} that is correctly classified by a quantum linear classifier $c \in \mathcal{C}_{\text{qlin}}^{(k)}$ with $0 < k < 2^n$, there exists a quantum linear classifier $c \in \mathcal{C}_{\text{qlin}}^{(r)}$ with $r > k$ that also correctly classifies \mathcal{D} .*
- (ii) *There exist a finite sets of examples that can be correctly classified by a classifier $c \in \mathcal{C}_{\text{qlin}}^{(r)}$, but which no classifier $c' \in \mathcal{C}_{\text{qlin}}^{(k)}$ with $k < r$ can classify correctly.*

The construction behind the proof of the above proposition is inspired by tomography of observables. Specifically, we construct a protocol that queries a quantum linear classifier and based on the assigned labels checks whether the underlying observable is approximately equal to a fixed target observable of a certain rank. In particular, we can use this to test whether the underlying observable is really of a given rank or not, as no low-rank observable can agree with a high-rank observable on the assigned labels during this protocol. Note that if we could query the expectation values of the observable, then tomography would be straightforward. However, the classifier only outputs the sign of the expectation value, which introduces a technical problem that we circumvent. Our protocol could be generalized to a more complete tomographic-protocol which uses queries to a quantum linear classifier in order to find the spectrum of the underlying observable.

Next, we investigate the effect that limitations of the rank of the observables used by a family of quantum linear classifier have on its ability to implement certain families of standard linear classifiers. In particular, assuming that the classical feature map is bounded (i.e., all feature vectors have a finite norm), then using the following proposition we can show that the following chain of inclusions holds:

$$\mathcal{C}_{\text{lin}} \text{ on } \mathbb{R}^{2^n} \subseteq \mathcal{C}_{\text{qlin}}^{(\leq 1)} \text{ on } n+1 \text{ qubits} \subseteq \cdots \subseteq \mathcal{C}_{\text{qlin}}^{(\leq r)} \text{ on } n+1 \text{ qubits} \subseteq \cdots \subseteq \mathcal{C}_{\text{lin}} \text{ on } \mathbb{R}^{4^n}, \quad (19)$$

where $\mathcal{C}_{\text{qlin}}^{(\leq r)}$ denotes the family of quantum linear classifiers using observables of rank at most r , and the inclusions mean that any function on the left-hand side can also be implemented by the right-hand side. We defer the proof to Appendix B.2.

Proposition 6. *Let $\mathcal{C}_{\text{lin}}(\Phi)$ denote the family of linear classifiers that is equipped with a feature map Φ . Also, let $\mathcal{C}_{\text{qlin}}^{(\leq r)}(\Phi')$ denote the family of quantum linear classifiers that uses observables of rank at most r and which is equipped with a quantum feature map Φ' . Then, the following statements hold:*

- (i) *For every feature map $\Phi : \mathbb{R}^\ell \rightarrow \mathbb{R}^N$ with $\sup_{x \in \mathbb{R}^\ell} \|\Phi(x)\| = M < \infty$, there exists a feature map $\Phi' : \mathbb{R}^\ell \rightarrow \mathbb{R}^{N+1}$ such that $\|\Phi'(x)\| = 1$ for all $x \in \mathbb{R}^\ell$ and the families of linear classifiers satisfy $\mathcal{C}_{\text{lin}}(\Phi) \subseteq \mathcal{C}_{\text{lin}}(\Phi')$.*
- (ii) *For every feature map $\Phi : \mathbb{R}^\ell \rightarrow \mathbb{R}^N$ with $\|\Phi(x)\| = 1$ for all $x \in \mathbb{R}^\ell$, there exists a quantum feature map $\Phi' : \mathbb{R}^\ell \rightarrow \text{Herm}(\mathbb{C}^{2^n})$ that uses $n = \lceil \log N + 1 \rceil + 1$ qubits such that the families of linear classifiers satisfy $\mathcal{C}_{\text{lin}}(\Phi) \subseteq \mathcal{C}_{\text{qlin}}^{(\leq 1)}(\Phi')$.*
- (iii) *For every quantum feature map $\Phi : \mathbb{R}^\ell \rightarrow \text{Herm}(\mathbb{C}^{2^n})$, there exists a classical feature map $\Phi' : \mathbb{R}^\ell \rightarrow \mathbb{R}^{4^n}$ such that the families of linear classifiers satisfy $\mathcal{C}_{\text{qlin}}(\Phi) = \mathcal{C}_{\text{lin}}(\Phi')$.*

Recall from the previous section that the fat-shattering dimension of a family of linear classifiers depends on the Frobenius norm of the observables that it uses. In the following proposition we investigate whether tuning the Frobenius norm changes the margins that the model can achieve, since larger margins give rise to better generalization performance (as discussed in Section 3.3). In particular, we show that there exist sets of examples that can only be classified with a certain margin by a classifier that uses an observable of at least a certain Frobenius norm. We defer the proof to Appendix B.3.

Proposition 7. Let $\mathcal{C}_{\text{qlin}}^{(\eta)}$ denote the family of quantum linear classifiers corresponding to all n -qubit observables of Frobenius norm η , that is,

$$\mathcal{C}_{\text{qlin}}^{(\eta)} = \left\{ c(\rho) = \text{sign}(\text{Tr}[\mathcal{O}\rho] - d) \mid \mathcal{O} \in \text{Herm}(\mathbb{C}^{2^n}) \text{ with } \|\mathcal{O}\|_F = \eta, d \in \mathbb{R} \right\}. \quad (20)$$

Then, for every $\eta \in \mathbb{R}_{>0}$ and $0 < m \leq 2^n$ there exists a set of m examples consisting of binary labeled n -qubit pure states that satisfies the following two conditions:

- (i) There exists a classifier $c \in \mathcal{C}_{\text{qlin}}^{(\eta)}$ that correctly classifies all examples with margin η/\sqrt{m} .
- (ii) No classifier $c' \in \mathcal{C}_{\text{qlin}}^{(\eta')}$ with $\eta' < \eta$ can classify all examples correctly with margin $\leq \eta/\sqrt{m}$.

In conclusion, Propositions 5 and 7 show that the rank and Frobenius norm of the observable used by the quantum linear classifier not only control the family's capacity – as shown in Propositions 1 and 2 – but that these model parameters also control its expressivity. However, note that tuning each model parameter actually achieves a different objective. Namely, increasing the rank of the observable increases the ability to correctly classify sets of examples, whereas increasing the Frobenius norm of the observable increases the margins that it can achieve. For example, one can increase the Frobenius norm of an observable by multiplying it with a positive scalar which increases the margin, but in order to correctly classify the sets of examples discussed in Proposition 5 one will really have to increase the rank of the observable.

3.4 Structural risk minimization for quantum linear classifiers in practice

Having established how certain model parameters of quantum linear classifiers influence both the model capacity and the ability to achieve small training errors, we now discuss how to use these results to implement structural risk minimization of quantum linear classifiers in practice. A common way to implement structural risk minimization is to add a so-called *regularization term* to your cost function that penalizes models with a larger model capacity. More specifically, while training the classifier you minimize a cost function of the form $E_{\text{train}} + h(\omega)$, where E_{train} denotes the error on the training examples, and h is a function that takes larger values for model parameters ω that correspond to more complex models. In this section, we discuss the types of regularization that can be performed in the context of quantum linear classifiers.

Firstly, recall that by tuning the rank of the observables used by a quantum linear classifier, we can balance the trade-off between its VC dimension and its ability to achieve small training errors. In particular, this shows that we can implement structural risk minimization of quantum linear classifiers with respect to the VC dimension by regularizing the rank of the observables. Moreover, recall from Section 3.3 that limiting the rank has a completely different effect on the expressivity compared to limiting the Frobenius norm (regularization of which we will discuss in the next paragraph). For explicit quantum linear classifiers, we can efficiently estimate the rank of the observable by sampling random computational basis states and computing the fraction that is not mapped to zero by the postprocessing function λ (note that in some cases the rank can be computed more directly). On the other hand, for implicit quantum linear classifiers, it is infeasible to implement the same regularization. This is due to the fact that estimating the rank of the implicit observable $\mathcal{O}_\alpha = \sum_{x \in \mathcal{D}} \alpha_x \rho_{\Phi(x)}$ requires estimating the dimension of the span of the feature vectors for which $\alpha_x \neq 0$, which can clearly become intractable for complex enough feature maps (moreover, the optimization of this is combinatorially hard). Nonetheless, one way to regularize rank of the

implicit observable to some extent is to regularize the weights α with respect to the 0-norm (i.e., the number of nonzero entries). Namely, as each ρ_x is of rank 1, we find that the rank of the implicit observable \mathcal{O}_α is at most $\|\alpha\|_0$. Finally, in these cases the regularized explicit and implicit quantum linear classifiers will give rise to different models without any theoretical guarantee regarding which will do better as the standard relationship between the two models [18] breaks down.

Secondly, recall that by tuning the Frobenius norms of the observables used by a quantum linear classifier, we can balance the trade-off between its fat-shattering dimension and its ability to achieve large margins. In particular, this shows that we can implement structural risk minimization of quantum linear classifiers with respect to the fat-shattering dimension by regularizing the Frobenius norms of the observables. As before, for explicit quantum linear classifiers, we can estimate the Frobenius norm by sampling random computational basis states and computing the average of the postprocessing function λ on them (note that in some cases the Frobenius norm can be computed more directly). On the other hand, for implicit quantum linear classifiers, if the weights are obtained by solving the usual quadratic program, then the resulting observable is already (optimally) regularized with respect to the Frobenius norm [18].

Besides the types of regularization for which we have established theoretical evidence of the effect on structural risk minimization, there are also other types of regularization that are important consider. For instance, for explicit quantum linear classifiers, one could regularize the angles of the parameterized quantum circuit [31]. Theoretically analyzing the effect that regularizing the angles of the parameterized quantum circuit has on structural risk minimization would constitute an interesting direction for future research. Another example is regularizing circuit parameters such as depth, width and number of gates for which certain theoretical results are known [22, 21]. Finally, it turns out that you can also regularize quantum linear classifiers by running the circuits under varying levels of noise [24]. For these kinds of regularization the relationships between the regularized explicit and regularized implicit quantum linear classifiers are still to be investigated.

Acknowledgments

The results of this work extend on the MSc thesis of Dyon van Vreumingen [30]. The authors thank Maria Schuld and Ryan Sweke for giving valuable comments on the manuscript. This work was supported by the Dutch Research Council (NWO/OCW), as part of the Quantum Software Consortium programme (project number 024.003.037).

References

- [1] Frank Arute, Kunal Arya, Ryan Babbush, Dave Bacon, Joseph C Bardin, Rami Barends, Ru-pak Biswas, Sergio Boixo, Fernando GSL Brandao, David A Buell, et al. Quantum supremacy using a programmable superconducting processor. *Nature*, 574, 2019.
- [2] John Preskill. Quantum computing in the NISQ era and beyond. *Quantum*, 2, 2018.
- [3] Marco Cerezo, Andrew Arrasmith, Ryan Babbush, Simon C Benjamin, Suguru Endo, Keisuke Fujii, Jarrod R McClean, Kosuke Mitarai, Xiao Yuan, Lukasz Cincio, et al. Variational quantum algorithms. *arXiv preprint arXiv:2012.09265*, 2020.
- [4] Jarrod R McClean, Jonathan Romero, Ryan Babbush, and Alán Aspuru-Guzik. The theory of variational hybrid quantum-classical algorithms. *New Journal of Physics*, 18, 2016.

- [5] Abhinav Kandala, Antonio Mezzacapo, Kristan Temme, Maika Takita, Markus Brink, Jerry M Chow, and Jay M Gambetta. Hardware-efficient variational quantum eigensolver for small molecules and quantum magnets. *Nature*, 549, 2017.
- [6] Alberto Peruzzo, Jarrod McClean, Peter Shadbolt, Man-Hong Yung, Xiao-Qi Zhou, Peter J Love, Alán Aspuru-Guzik, and Jeremy L O'brien. A variational eigenvalue solver on a photonic quantum processor. *Nature communications*, 5, 2014.
- [7] Peter JJ O'Malley, Ryan Babbush, Ian D Kivlichan, Jonathan Romero, Jarrod R McClean, Rami Barends, Julian Kelly, Pedram Roushan, Andrew Tranter, Nan Ding, et al. Scalable quantum simulation of molecular energies. *Physical Review X*, 6, 2016.
- [8] Edward Farhi, Jeffrey Goldstone, and Sam Gutmann. A quantum approximate optimization algorithm. *arXiv preprint arXiv:1411.4028*, 2014.
- [9] Marcello Benedetti, Erika Lloyd, Stefan Sack, and Mattia Fiorentini. Parameterized quantum circuits as machine learning models. *Quantum Science and Technology*, 4, 2019.
- [10] Barbara M Terhal and David P DiVincenzo. Adaptive quantum computation, constant depth quantum circuits and arthur-merlin games. *Quantum Information & Computation*, 4, 2004.
- [11] Michael J Bremner, Richard Jozsa, and Dan J Shepherd. Classical simulation of commuting quantum computations implies collapse of the polynomial hierarchy. *Proceedings of the Royal Society A: Mathematical, Physical and Engineering Sciences*, 467, 2011.
- [12] Edward Grant, Marcello Benedetti, Shuxiang Cao, Andrew Hallam, Joshua Lockhart, Vid Stojevic, Andrew G Green, and Simone Severini. Hierarchical quantum classifiers. *npj Quantum Information*, 4, 2018.
- [13] Diego Ristè, Marcus P Da Silva, Colm A Ryan, Andrew W Cross, Antonio D Córdcoles, John A Smolin, Jay M Gambetta, Jerry M Chow, and Blake R Johnson. Demonstration of quantum advantage in machine learning. *npj Quantum Information*, 3, 2017.
- [14] Vojtěch Havlíček, Antonio D Córdcoles, Kristan Temme, Aram W Harrow, Abhinav Kandala, Jerry M Chow, and Jay M Gambetta. Supervised learning with quantum-enhanced feature spaces. *Nature*, 567, 2019.
- [15] Maria Schuld and Nathan Killoran. Quantum machine learning in feature Hilbert spaces. *Physical review letters*, 122, 2019.
- [16] Mehryar Mohri, Afshin Rostamizadeh, and Ameet Talwalkar. *Foundations of machine learning*. MIT press, 2018.
- [17] Peter L Bartlett. The sample complexity of pattern classification with neural networks: the size of the weights is more important than the size of the network. *IEEE transactions on Information Theory*, 44, 1998.
- [18] Maria Schuld. Quantum machine learning models are kernel methods. *arXiv preprint arXiv:2101.11020*, 2021.

- [19] Logan G Wright and Peter L McMahon. The capacity of quantum neural networks. In *CLEO: QELS_Fundamental Science*. Optical Society of America, 2020.
- [20] Amira Abbas, David Sutter, Christa Zoufal, Aurélien Lucchi, Alessio Figalli, and Stefan Woerner. The power of quantum neural networks. *arXiv preprint arXiv:2011.00027*, 2020.
- [21] Matthias C Caro and Ishaun Datta. Pseudo-dimension of quantum circuits. *Quantum Machine Intelligence*, 2, 2020.
- [22] Kaifeng Bu, Dax Enshan Koh, Lu Li, Qingxian Luo, and Yaobo Zhang. On the statistical complexity of quantum circuits. *arXiv preprint arXiv:2101.06154*, 2021.
- [23] Kaifeng Bu, Dax Enshan Koh, Lu Li, Qingxian Luo, and Yaobo Zhang. Effects of quantum resources on the statistical complexity of quantum circuits. *arXiv preprint arXiv:2102.03282*, 2021.
- [24] Kaifeng Bu, Dax Enshan Koh, Lu Li, Qingxian Luo, and Yaobo Zhang. Rademacher complexity of noisy quantum circuits. *arXiv preprint arXiv:2103.03139*, 2021.
- [25] Hsin-Yuan Huang, Michael Broughton, Masoud Mohseni, Ryan Babbush, Sergio Boixo, Hartmut Neven, and Jarrod R McClean. Power of data in quantum machine learning. *arXiv preprint arXiv:2011.01938*, 2020.
- [26] Hsin-Yuan Huang, Richard Kueng, and John Preskill. Information-theoretic bounds on quantum advantage in machine learning. *arXiv preprint arXiv:2101.02464*, 2021.
- [27] Yunchao Liu, Srinivasan Arunachalam, and Kristan Temme. A rigorous and robust quantum speed-up in supervised machine learning. *arXiv preprint arXiv:2010.02174*, 2020.
- [28] Vladimir N Vapnik and A Ya Chervonenkis. On the uniform convergence of relative frequencies of events to their probabilities. In *Measures of complexity*. Springer, 2015.
- [29] Michael J Kearns and Robert E Schapire. Efficient distribution-free learning of probabilistic concepts. *Journal of Computer and System Sciences*, 48, 1994.
- [30] Dyon van Vreumingen. Quantum feature space learning: characterisation and possible advantages. Master's thesis, Leiden University, 8 2020. <https://studenttheses.universiteitleiden.nl/handle/1887/2734545>.
- [31] Jae-Eun Park, Brian Quanz, Steve Wood, Heather Higgins, and Ray Harishankar. Practical application improvement to quantum svm: theory to practice. *arXiv preprint arXiv:2012.07725*, 2020.
- [32] John Shawe-Taylor, Peter L. Bartlett, Robert C. Williamson, and Martin Anthony. Structural risk minimization over data-dependent hierarchies. *IEEE Transactions on Information Theory*, 1998.
- [33] Christopher J C Burges. A tutorial on support vector machines for pattern recognition. *Data Min. Knowl. Discov.*, 2, 1998.

- [34] Martin Anthony and Peter L Bartlett. Function learning from interpolation. *Combinatorics, Probability and Computing*, 9, 2000.
- [35] Peter L Bartlett and Philip M Long. Prediction, learning, uniform convergence, and scale-sensitive dimensions. *Journal of Computer and System Sciences*, 56, 1998.
- [36] Scott Aaronson. The learnability of quantum states. *Proceedings of the Royal Society A: Mathematical, Physical and Engineering Sciences*, 2007. quant-ph/0608142.
- [37] Semyon Aranovich Gershgorin. Über die Abgrenzung der Eigenwerte einer Matrix. *Bulletin of the Russian Academy of Sciences*, (6), 1931.

A Proofs of propositions Section 3.2

A.1 Proof of Proposition 3

Proposition 3. Let $\mathbb{O} \subseteq \text{Herm}(\mathbb{C}^{2^n})$ be a family of n -qubit observables with $r = \dim(\sum_{\mathcal{O} \in \mathbb{O}} \text{Im } \mathcal{O})$ ⁴. Then, the VC dimension of

$$\mathcal{C}_{\text{qlin}}^{\mathbb{O}} = \left\{ c(\rho) = \text{sign}(\text{Tr}[\mathcal{O}\rho] - d) \mid \mathcal{O} \in \mathbb{O}, d \in \mathbb{R} \right\} \quad (14)$$

is upper bounded by

$$\text{VC}(\mathcal{C}_{\text{qlin}}^{\mathbb{O}}) \leq r + 1. \quad (15)$$

Proof. Define $V = \sum_{\mathcal{O} \in \mathbb{O}} \text{Im } \mathcal{O} \subset \mathbb{C}^{2^n}$ and let P_V denote the orthogonal projector onto V . Let $\Phi : \mathcal{X} \rightarrow \text{Herm}(\mathbb{C}^{2^n})$ denote the feature map of $\mathcal{C}_{\text{qlin}}^{\mathbb{O}}$ and define $\Phi' = P_V \Phi P_V$. Note that the image of Φ' is r -dimensional and that $\mathcal{C}_{\text{qlin}}^{\mathbb{O}}(\Phi') = \mathcal{C}_{\text{qlin}}^{\mathbb{O}}(\Phi)$. Finally, it is known that the VC dimension of standard linear classifiers on \mathbb{R}^r is equal to $r + 1$. We therefore conclude that

$$\text{VC}(\mathcal{C}_{\text{qlin}}^{\mathbb{O}}(\Phi)) = \text{VC}(\mathcal{C}_{\text{qlin}}^{\mathbb{O}}(\Phi')) \leq \text{VC}(\text{linear classifiers on } \mathbb{R}^r) = r + 1.$$

□

A.2 Proof of Proposition 4

Proposition 4. Let $\mathbb{O} \subseteq \text{Herm}(\mathbb{C}^{2^n})$ be a family of n -qubit observables with $\eta = \max_{\mathcal{O} \in \mathbb{O}} \|\mathcal{O}\|_F$. Then, the fat-shattering dimension of

$$\mathcal{F}_{\text{qlin}}^{\mathbb{O}} = \left\{ f_{\mathcal{O}, d}(\rho) = \text{Tr}[\mathcal{O}\rho] - d \mid \mathcal{O} \in \mathbb{O}, d \in \mathbb{R} \right\} \quad (16)$$

is upper bounded by

$$\text{fat}_{\mathcal{F}_{\text{qlin}}^{\mathbb{O}}}(\gamma) \leq O\left(\frac{\eta^2}{\gamma^2}\right). \quad (17)$$

Proof. Due to the close relationship to standard linear classifiers, we can utilize previously obtained results in that context. In particular, for our approach we use the following proposition.

Proposition 8 (Fat-shattering dimension of linear functions [32]). *Consider the family of real-valued functions on the ball of radius R inside \mathbb{R}^N given by*

$$\mathcal{F}_{\text{lin}} = \left\{ f_{w, d}(x) = \langle w, x \rangle - d \mid w \in \mathbb{R}^N \text{ with } \|w\| = 1, d \in \mathbb{R} \text{ with } |d| \leq R \right\}.$$

The fat-shattering dimension of \mathcal{F}_{lin} can be bounded by

$$\text{fat}_{\mathcal{F}_{\text{lin}}}(\gamma) \leq \min\{9R^2/\gamma^2, N + 1\} + 1.$$

⁴Here \sum denotes the sum of vector spaces.

The context in the above proposition is indeed closely related, yet slightly different than that of quantum linear classifiers. Firstly, n -qubit density matrices lie within the ball of radius $R = 1$ inside the vector space of n -qubit Hermitian operators equipped with the Frobenius norm. However, as in our case the hyperplanes arise from the family of observables \mathbb{O} , whose Frobenius norms are generally not equal to 1 (e.g., in the explicit model this is related to the function λ , and in the implicit model this is related to the magnitudes of the weights α), we cannot directly apply the above proposition. We therefore adapt the above proposition by exchanging the role of R with an upper bound on the norms of the observables in \mathbb{O} , resulting in the following lemma.

Lemma 9. *Consider the family of real-valued functions on the ball of radius $R = 1$ inside \mathbb{R}^N given by*

$$\mathcal{F}_{\text{lin}}^{\leq \eta} = \left\{ f_{w,d}(x) = \langle w, x \rangle - d \mid w \in \mathbb{R}^N \text{ with } \|w\| \leq \eta, d \in \mathbb{R} \text{ with } |d| \leq \eta \right\}.$$

The fat shattering dimension of $\mathcal{F}_{\text{lin}}^{\leq \eta}$ can be upper bounded by

$$\text{fat}_{\mathcal{F}_{\text{lin}}^{\leq \eta}}(\gamma) \leq \min\{9\eta^2/\gamma^2, N + 1\} + 1.$$

Proof. Let us first determine the fat-shattering dimension of the family of linear functions with norm precisely equal to η on points that lie within the ball of radius $R = 1$, i.e.,

$$\mathcal{F}_{\text{lin}}^{=\eta} = \left\{ f_{w,d}(x) = \langle w, x \rangle - d \mid w \in \mathbb{R}^N \text{ with } \|w\| = \eta, d \in \mathbb{R} \text{ with } |d| \leq \eta \right\}.$$

To do so, suppose $\mathcal{F}_{\text{lin}}^{=\eta}$ can γ -shatter a set of points $\{x_1, \dots, x_k\}$ that lie within the ball of radius $R = 1$. Because $\langle w, x_i \rangle = \langle w/\eta, \eta x_i \rangle$, we find that $\mathcal{F}_{\text{lin}}^{=1}$ can γ -shatter the set of points $\eta x_1, \dots, \eta x_k$ that lie within the ball of radius $R = \eta$. By Proposition 8 we have $k \leq \min\{9\eta^2/\gamma^2, N + 1\} + 1$. In particular, the fat-shattering dimension of $\mathcal{F}_{\text{lin}}^{=\eta}$ on points within the ball of radius $R = 1$ is upper bounded by

$$\text{fat}_{\mathcal{F}_{\text{lin}}^{=\eta}}(\gamma) \leq \min\{9\eta^2/\gamma^2, N + 1\} + 1.$$

To conclude the desired results, note that this bound is monotonically increasing in η , and thus allowing hyperplanes with norm $\|w\| < \eta$ will not increase the fat-shattering dimension. \square

From the above lemma we can immediately infer an upper bound on the fat-shattering dimension of quantum linear classifiers by identifying the vector space of n -qubit Hermitian operators equipped with the Frobenius inner product as a real vector space of dimension 4^n . \square

A.2.1 Sample complexity in the PAC-learning framework

Besides being related to generalization performance, the fat-shattering dimension is also related to the so-called *sample complexity* in the probably approximately correct (PAC) learning framework [29]. The sample complexity captures the amount classifier queries required to find another classifier that with high probability agrees with the former classifier on unseen examples. However, in this context a lower bound on the fat-shattering dimension is required.

Proposition 10. Let $\eta \in \mathbb{R}_{>0}$. Then, the fat-shattering dimension of

$$\mathcal{F}_{\text{qlin}}^{(\eta)} = \left\{ f(\rho) = \text{sign}(\text{Tr}[\mathcal{O}\rho] - d) \mid \mathcal{O} \in \text{Herm}(\mathbb{C}^{2^n}) \text{ with } \|\mathcal{O}\|_F \leq \eta, d \in \mathbb{R} \right\} \subseteq \mathcal{F}_{\text{qlin}}. \quad (21)$$

can be lower bounded by

$$\text{fat}_{\mathcal{F}_{\text{qlin}}^{(\eta)}}(\gamma) \geq \min\{\eta^2(1 - 2^{-n})/\gamma^2, 2^n\}.$$

Proof. We show that quantum linear classifiers can shatter a set of points on a symmetric simplex whose size is equal to the lower bound provided in Proposition 10 using the following lemma.

Lemma 11. Let ϕ_1, \dots, ϕ_N be points of unit norm in \mathbb{R}^{N-1} , with $N = 2^n$, that form the vertices of a symmetric $(N-1)$ -simplex. Suppose the set

$$\mathcal{F}_{\text{lin}}^{=\eta} = \left\{ f_{w,d}(x) = \langle w, x \rangle - d \mid w \in \mathbb{R}^{N-1} \text{ with } \|w\| = \eta, d \in \mathbb{R} \right\}$$

can γ -shatter the set points ϕ_1, \dots, ϕ_k for some $k \leq N$. Then, the set of functions underlying a quantum linear classifier given by

$$\mathcal{F}_{\text{qlin}}^{=u_N\eta} = \left\{ f_{\mathcal{O},d}(\rho) = \text{Tr}[\mathcal{O}\rho] - d \mid \mathcal{O} \in \text{Herm}(\mathbb{C}^N) \text{ with } \|\mathcal{O}\|_F = u_N\eta, d \in \mathbb{R} \right\}$$

where $u_N = 1/\sqrt{1 - 1/N}$, can γ -shatter the set of n -qubit pure states ρ_1, \dots, ρ_k , with $\rho_i = |i\rangle\langle i|$.

Proof. Suppose a function $f = f_{w,d} \in \mathcal{F}_{\text{lin}}^{\eta}$ separates ϕ_1, \dots, ϕ_k by margin γ under assignment y and offset s , that is,

$$\langle f, \phi_i \rangle \begin{cases} \leq s_i - \gamma & \text{if } y_i = -1, \\ \geq s_i + \gamma & \text{if } y_i = +1. \end{cases}$$

Consider the set $\mathcal{F}_{\text{lin}}^{=u_N\eta}$ of linear functions on \mathbb{R}^N with norm $u_N\eta$, where $u_N = 1/\sqrt{1 - 1/N}$. Define the vector $w' \in \mathbb{R}^N$ with entries $w'_i = \langle f, \phi_i \rangle$. This vector has norm $u_N\eta$, since the ϕ_i satisfy

$$\langle \phi_i, \phi_j \rangle = -1/(N-1), \quad \text{for } i \neq j,$$

which shows that $f' = f_{w',d} \in \mathcal{F}_{\text{lin}}^{=u_N\eta}$. Moreover, let e_i denote the i -th standard basis vector in \mathbb{R}^N and note that f' can γ -separate the set e_1, \dots, e_k under assignment y and offset s , since $\langle w', e_i \rangle = \langle w, \phi_i \rangle$. Lastly, consider the n -qubit observable $\mathcal{O} = \text{diag}(w'_1, \dots, w'_N)$ and note that $\|\mathcal{O}\|_F = \|f'\| = u_N\eta$, so $f_{\mathcal{O},d} \in \mathcal{F}_{\text{qlin}}^{=u_N\eta}$. Moreover, since $\text{Tr}[\mathcal{O}\rho_i] = \langle w', e_i \rangle$, we find that $f_{\mathcal{O},d}$ can γ -shatter the pure states ρ_1, \dots, ρ_k . In conclusion, if $\mathcal{F}_{\text{lin}}^{=\eta}$ can γ -shatter ϕ_1, \dots, ϕ_k , then $\mathcal{F}_{\text{qlin}}^{=u_N\eta}$ can γ -shatter ρ_1, \dots, ρ_k .

□

To proof the desired result we now invoke a result of Burges [33] on the number of points on a symmetric simplex that a standard linear classifier can shatter, which states that the family of functions

$$\mathcal{F}_{\text{lin}}^{=1} = \left\{ f_{w,d}(x) = \langle w, x \rangle - d \mid w \in \mathbb{R}^{N-1} \text{ with } \|w\| = 1, d \in \mathbb{R} \right\}$$

can γ -shatter k vertices of a symmetric $(N-1)$ -simplex lying on a sphere of radius ν if

$$\nu^2/\gamma^2 \geq k - 1.$$

Therefore, the set $\mathcal{F}_{\text{lin}}^{=\nu}$ can γ -shatter k vertices of a symmetric $(N-1)$ -simplex lying on the unit sphere under the same condition. Combining this with Lemma 11 we find that k orthogonal n -qubit pure states $|i\rangle\langle i|$ can be γ -shattered by the family $\mathcal{F}_{\text{qlin}}^{=\eta}$ of n -qubit observables with norm η , if $\eta^2/u_N^2\gamma^2 \geq k-1$, where $u_N = 1/\sqrt{1-1/N}$. Hence, the maximum number of pure states $|i\rangle\langle i|$ that can be γ -shattered by $\mathcal{F}_{\text{qlin}}^{=\eta}$ is $\lfloor \eta^2/u_N^2\gamma^2 \rfloor + 1$. Since we can have at most $N = 2^n$ orthogonal n -qubit pure states, we find that the fat shattering dimension of $\mathcal{F}_{\text{qlin}}^{=\eta}$ is lower bounded by

$$\text{fat}_{\mathcal{F}_{\text{qlin}}^{=\eta}}(\gamma) \geq \min\{\eta^2(1-2^{-n})/\gamma^2, 2^n\}.$$

Since this function is strictly increasing in η , allowing observables with norm larger than ν does not decrease the fat shattering dimension. \square

By plugging the above lower bound into previously established theorems on the sample complexity of families of classifiers [34, 35], we derive the following corollary, which can be viewed as a dual of the result of [36].

Corollary 12. *Consider the family of real-valued functions $\mathcal{F}_{\text{qlin}}^{(\eta)}$ defined in Equation (21). Fix an element $F \in \mathcal{F}_{\text{qlin}}^{(\eta)}$ as well as parameters $\varepsilon, \nu, \gamma > 0$ with $\gamma\varepsilon \geq 7\nu$ and $((35\eta)^2(1-2^{-n}))/\gamma^2\varepsilon^2 < 2^n$. Suppose we draw m examples $\mathcal{D} = \{\rho_1, \dots, \rho_m\}$ independently according to a distribution P , and then choose any function $H \in \mathcal{F}_{\text{qlin}}^{(\eta)}$ such that $|H(\rho_i) - F(\rho_i)| \leq \nu$ for all $\rho_i \in \mathcal{D}$. Then, with probability at least $1 - \delta$ over P , we have that*

$$\Pr_{\rho \sim P}(|H(\rho) - F(\rho)| > \gamma) \leq \varepsilon,$$

provided that

$$m \in \Omega\left(\frac{1}{\gamma^2\varepsilon^2} \left(\frac{\eta^2(1-2^{-n})}{\gamma^2\varepsilon^2} \log^2 \frac{1}{\gamma\varepsilon} + \log \frac{1}{\delta} \right)\right).$$

Proof. Follows directly from plugging the lower bound of Proposition 10 into Corollary 2.4 of [36]. \square

B Proofs of propositions Section 3.3

B.1 Proof of Proposition 5

Proposition 5. *Let $\mathcal{C}_{\text{qlin}}^{(r)}$ denote the family of quantum linear classifiers corresponding to observables of rank r , that is,*

$$\mathcal{C}_{\text{qlin}}^{(r)} = \left\{ c(\rho) = \text{sign}(\text{Tr}[\mathcal{O}\rho] - d) \mid \mathcal{O} \in \text{Herm}(\mathbb{C}^{2^n}), \text{rank}(\mathcal{O}) = r, d \in \mathbb{R} \right\} \quad (18)$$

Then, the following statements hold:

- (i) *For every finite set of examples \mathcal{D} that is correctly classified by a quantum linear classifier $c \in \mathcal{C}_{\text{qlin}}^{(k)}$ with $0 < k < 2^n$, there exists a quantum linear classifier $c \in \mathcal{C}_{\text{qlin}}^{(r)}$ with $r > k$ that also correctly classifies \mathcal{D} .*

(ii) There exist a finite sets of examples that can be correctly classified by a classifier $c \in \mathcal{C}_{\text{qlin}}^{(r)}$, but which no classifier $c' \in \mathcal{C}_{\text{qlin}}^{(k)}$ with $k < r$ can classify correctly.

Proof. (i): Suppose $c_{\mathcal{O},b} \in \mathcal{C}_{\text{qlin}}^{(k)}$ correctly classifies \mathcal{D} . Let $\delta = \min_{x \in \mathcal{D}_-} |\text{Tr}[\mathcal{O}\rho_x] - b|$, where \mathcal{D}_- is the subset of examples with label -1 , and note that since \mathcal{D} is correctly classified we have $\delta > 0$. Fix the basis we work in to be the eigenbasis of \mathcal{O} ordered in such a way that

$$\mathcal{O} = \text{diag}(\lambda_1, \dots, \lambda_k, 0, \dots, 0)$$

and define

$$P = \frac{1}{r-k} \text{diag}(\underbrace{0, \dots, 0}_{k \text{ times}}, \underbrace{1, \dots, 1}_{r-k \text{ times}}, \underbrace{0, \dots, 0}_{2^n-r \text{ times}}).$$

Now for every $0 < \varepsilon < \delta$ we have that $\mathcal{O}' = \mathcal{O} + \varepsilon P$ has $\text{rank}(\mathcal{O}') = r$. What remains to be shown is that $c_{\mathcal{O}',b} \in \mathcal{C}_{\text{qlin}}^{(r)}$ also correctly classifies \mathcal{D} . To do so, first let $x \in \mathcal{D}_+$ (i.e., labeled $+1$) and note that

$$\text{Tr}[\mathcal{O}'\rho_x] - b = \underbrace{(\text{Tr}[\mathcal{O}\rho_x] - b)}_{\geq 0} + \underbrace{\varepsilon \text{Tr}[P\rho_x]}_{\geq 0} \geq 0,$$

which shows that indeed $c_{\mathcal{O}',b}(x) = +1$. Next, let $x \in \mathcal{D}_-$ (i.e., labeled -1) and note that

$$\text{Tr}[\mathcal{O}'\rho_x] - b = \underbrace{(\text{Tr}[\mathcal{O}\rho_x] - b)}_{\leq -\delta} + \underbrace{\varepsilon \text{Tr}[P\rho_x]}_{< \delta} < 0,$$

which shows that indeed $c_{\mathcal{O}',b}(x) = -1$.

(ii): We will describe a protocol that queries a classifier $c_{\mathcal{O},b}$ and based on its outcomes checks whether \mathcal{O} is approximately equal to a fixed target observable \mathcal{T} of rank r . We will show that if the queries are labeled in a way that agrees with the target classifier that uses the observable \mathcal{T} , then the spectrum of \mathcal{O} has to be point-wise within distance ε of the spectrum of \mathcal{T} . In particular, this will show that the rank of \mathcal{O} has to be at least r if we make ε small enough. Consequentially, if the rank of \mathcal{O} is less than r , then at least one query made during the protocol has to be labeled different by $c_{\mathcal{O},b}$ than the target classifier. In the end, the queries made to the classifier during the protocol will therefore constitute the set of examples described in the theorem.

Let us start with some definition. For a classifier $c_{\mathcal{O},b}(\rho) = \text{sgn}(\text{Tr}[\mathcal{O}\rho] - b)$ we define its effective observable $\mathcal{O}_{\text{eff}} = \mathcal{O} - bI$ which we express in the computational basis as $\mathcal{O}_{\text{eff}} = (O_{ij})$. Next, we define our target classifier to be $c_{\mathcal{T},-1}$ where the observable \mathcal{T} is given by

$$\mathcal{T} = -r \cdot |0\rangle\langle 0| + \sum_{i=1}^{r-1} i \cdot |i\rangle\langle i|,$$

and we define its effective observable $\mathcal{T}_{\text{eff}} = \mathcal{T} + I$ which we express in the computational basis as $\mathcal{T}_{\text{eff}} = (T_{ij})$. Rescaling \mathcal{O}_{eff} with a positive scalar does not change the output of the corresponding classifier. Therefore, to make the protocol well-defined, we define \mathcal{O}_{eff} to be the unique effective observable whose first diagonal element is scaled to be equal to $O_{00} = -(r+1)$.

Our approach is as follows. First, we query $c_{\mathcal{O},b}$ in such a way that if the outcomes agree with with the target classifier $c_{\mathcal{T},-1}$, then the absolute values of the off-diagonal entries in the first row

and column of \mathcal{O}_{eff} must be close to zero (i.e., approximately equal to those of \mathcal{T}_{eff}). Afterwards, we again query $c_{\mathcal{O},b}$ but now in such a way that if the outcomes agree with the target classifier $c_{\mathcal{T},-1}$, then the diagonal elements of \mathcal{O}_{eff} must be approximately equal to those of \mathcal{T}_{eff} . In the end, we query $c_{\mathcal{O},b}$ one final time but this time in such a way that if the outcomes agree with the target classifier $c_{\mathcal{T},-1}$, then the absolute values of the remaining off-diagonal elements of \mathcal{O}_{eff} must be close to zero (i.e., again approximately equal to those of \mathcal{T}_{eff}). Finally, we use Gershgorin's circle theorem [37] to show that the spectrum of \mathcal{O}_{eff} has to be point-wise close to the spectrum of \mathcal{T}_{eff} . We remark that this procedure could be generalized to a more complete tomography approach, where one uses queries to the classifier $c_{\mathcal{O},b}$ in order to estimate the eigenvalues of \mathcal{O}_{eff} .

To begin with, we query the quantum states $|i\rangle$ for $i = 0, \dots, 2^n - 1$. Without loss of generality, we can assume that the classifiers $c_{\mathcal{O},b}$ and $c_{\mathcal{T},-1}$ agree on the label, i.e.,

$$c_{\mathcal{O},b}(|0\rangle\langle 0|) = -1, \text{ and } c_{\mathcal{O},b}(|i\rangle\langle i|) = +1 \text{ for } i = 1, \dots, 2^n - 1, \quad (22)$$

as otherwise a set of examples containing just these states would already separate $c_{\mathcal{O},b}$ and $c_{\mathcal{T},-1}$.

In order to show that the absolute value of the off-diagonal elements of the first row and column of \mathcal{O}_{eff} must be close to zero and that the diagonal elements of \mathcal{O}_{eff} must be close to those of \mathcal{T}_{eff} , we consider the quantum states given by

$$|\gamma_\theta(\alpha)\rangle = \sqrt{1-\alpha}|0\rangle + e^{i\theta}\sqrt{\alpha}|j\rangle, \quad \text{with } \alpha \in [0, 1] \text{ and } \theta \in [0, 2\pi]. \quad (23)$$

Its expectation value with respect to \mathcal{O}_{eff} is given by

$$\langle \gamma_\theta(\alpha) | \mathcal{O}_{\text{eff}} | \gamma_\theta(\alpha) \rangle = (1-\alpha) \cdot O_{00} + \alpha \cdot O_{jj} + \sqrt{\alpha(1-\alpha)} \cdot C_\theta, \quad \text{where } C_\theta := \text{Re}(e^{i\theta} O_{0j}), \quad (24)$$

and its expectation value with respect to \mathcal{T}_{eff} is given by

$$\langle \gamma_\theta(\alpha) | \mathcal{T}_{\text{eff}} | \gamma_\theta(\alpha) \rangle = (1-\alpha) \cdot T_{00} + \alpha \cdot T_{jj}. \quad (25)$$

Crucially, by Equation (22) we know that the label of $|\gamma_\theta(\alpha)\rangle$ goes from -1 to $+1$ as α goes $0 \rightarrow 1$. Note that the expectation value of $|\gamma_\theta(\alpha)\rangle$ with respect to \mathcal{T}_{eff} is independent from the phase θ .

To determine that $|O_{0j}|$ is smaller than $\delta > 0$, we query the classifier $c_{\mathcal{O},b}$ on the states $|\gamma_{\hat{\theta}}(\hat{\alpha})\rangle$ for all $\hat{\theta}$ in a ζ -mesh of $[0, 2\pi)$ and for all $\hat{\alpha}$ in a ξ -mesh of $[0, 1]$ and we suppose they are labeled the same as the target classifier $c_{\mathcal{T},-1}$ would label them. Using these queries we can find estimates $\hat{\alpha}_{\text{cross}}^{\mathcal{O}_{\text{eff}}}(\hat{\theta})$ that are ξ -close to the unique $\alpha_{\text{cross}}^{\mathcal{O}_{\text{eff}}}(\theta) = \alpha'$ that satisfies

$$\langle \gamma_\theta(\alpha') | \mathcal{O}_{\text{eff}} | \gamma_\theta(\alpha') \rangle = 0, \quad (26)$$

by finding the smallest $\hat{\alpha}$ where the label has gone from -1 to $+1$. We refer to the α' satisfying Equation (26) as the *crossing point at phase θ* . Because the label assigned by $c_{\mathcal{T},-1}$ does not depend on the phase θ , and since all states $|\gamma_{\hat{\theta}}(\hat{\alpha})\rangle$ were assigned the same label by $c_{\mathcal{O},b}$ and $c_{\mathcal{T},-1}$, we find that the crossing point estimate $\hat{\alpha}_{\text{cross}}^{\mathcal{O}_{\text{eff}}}(\hat{\theta})$ is the same for all $\hat{\theta}$. In particular, this implies that the actual crossing points $\alpha_{\text{cross}}^{\mathcal{O}_{\text{eff}}}(\hat{\theta})$ have to be within ξ -distance of each other for all $\hat{\theta}$. Subsequently, write $O_{0j} = |O_{0j}|e^{i\phi}$ with $\phi \in [0, 2\pi)$, let $\hat{\theta}_{\text{abs}}$ denote the point in the ζ -mesh of $[0, 2\pi)$ that is closest to $2\pi - \phi$, and let $\hat{\theta}_0$ denote the point in the ζ -mesh of $[0, 2\pi)$ that is closest to $\pi/2 - \phi$ modulo 2π . By our previous discussion we know that $|\alpha_{\text{cross}}^{\mathcal{O}_{\text{eff}}}(\hat{\theta}_{\text{abs}}) - \alpha_{\text{cross}}^{\mathcal{O}_{\text{eff}}}(\hat{\theta}_0)| < \xi$, which implies

$$|C_{\hat{\theta}_{\text{abs}}} - C_{\hat{\theta}_0}| < f(\xi), \quad (27)$$

where f is a continuous function (independent from $c_{\mathcal{O},b}$ and $c_{\mathcal{T},-1}$) with $f(\xi) \rightarrow 0$ as $\xi \rightarrow 0$. Moreover, using the inequality $\cos(\zeta) \geq 1 - \lambda\zeta$, where $\lambda \approx 0.7246$ is a solution of $\lambda(\pi - \arcsin(\lambda)) = 1 + \sqrt{1 - \lambda^2}$, together with the inequality $\cos(\pi/2 - \zeta) \leq \zeta$, we can derive that

$$\begin{aligned} |C_{\hat{\theta}_{\text{abs}}} - C_{\hat{\theta}_0}| &= \left| |O_{0j}| \cos(\hat{\theta}_{\text{abs}} + \phi) - |O_{0j}| \cos(\hat{\theta}_0 + \phi) \right| \\ &\geq |O_{0j}| \cdot \left| \cos(\zeta) - \cos(\pi/2 - \zeta) \right| \\ &\geq |O_{0j}| \cdot \left| 1 - (\lambda + 1)\zeta \right|. \end{aligned} \quad (28)$$

Finally, by combining Equation (27) with Equation (28) we can conclude that

$$|O_{0j}| < \frac{f(\xi)}{1 - (\lambda + 1)\zeta},$$

which for ξ and ζ small enough shows that $|O_{0j}| < \delta$ for any chosen precision $\delta > 0$ (i.e., the fineness of both meshes ξ and ζ will depend on the choice of δ).

To determine that O_{jj} is within distance $\delta' > 0$ of T_{jj} we again query the classifier $c_{\mathcal{O},b}$ but this time on the states $|\gamma_0(\hat{\alpha})\rangle$ for all $\hat{\alpha}$ in a ξ' -mesh of $[0, 1]$ and we suppose they are labeled the same as the target classifier $c_{\mathcal{T},-1}$ would. Using these queries we can find an estimate $\hat{\alpha}_{\text{cross}}^{\mathcal{O}_{\text{eff}}}(0)$, $\hat{\alpha}_{\text{cross}}^{\mathcal{T}_{\text{eff}}}(0)$ that are ξ' -close to the corresponding actual crossing point. As we assumed that all queries are labeled the same by $c_{\mathcal{O},b}$ and $c_{\mathcal{T},-1}$, the crossing point estimate $\hat{\alpha}_{\text{cross}}^{\mathcal{O}_{\text{eff}}}(0)$ has to be equal to the crossing point estimate $\hat{\alpha}_{\text{cross}}^{\mathcal{T}_{\text{eff}}}(0)$. In particular, this implies that the actual crossing points $\alpha_{\text{cross}}^{\mathcal{O}_{\text{eff}}}(0)$ and $\alpha_{\text{cross}}^{\mathcal{T}_{\text{eff}}}(0)$ have to be within ξ' -distance of each other. Next, define $g(\alpha, C)$ to be the unique coefficient $O \in \mathbb{R}_{\geq 0}$ that satisfies

$$(1 - \alpha) \cdot O_{00} + \alpha \cdot O + \sqrt{\alpha(1 - \alpha)} \cdot C = 0.$$

It is clear that g is a continuous function in α and C that is independent from $c_{\mathcal{O},b}$ and $c_{\mathcal{T},-1}$, and that $T_{jj} = g(\alpha_{\text{cross}}^{\mathcal{T}_{\text{eff}}}(0), 0)$ and $O_{jj} = g(\alpha_{\text{cross}}^{\mathcal{O}_{\text{eff}}}(0), C_0)$. Finally, we let $\delta > 0$ and $\xi' > 0$ be small enough such that if $|\alpha_{\text{cross}}^{\mathcal{O}_{\text{eff}}}(0) - \alpha_{\text{cross}}^{\mathcal{T}_{\text{eff}}}(0)| < \xi'$ and $|C_0| < \delta$, then

$$|O_{jj} - T_{jj}| = |g(\alpha_{\text{cross}}^{\mathcal{T}_{\text{eff}}}(0), 0) - g(\alpha_{\text{cross}}^{\mathcal{O}_{\text{eff}}}(0), C_0)| < \delta'.$$

In conclusion, to determine that O_{jj} is within distance $\delta' > 0$ of T_{jj} we first do the required queries to determine that $|C_0| = |O_{0j}| < \delta$, after which we do the required queries to determine that $|\alpha_{\text{cross}}^{\mathcal{O}_{\text{eff}}}(0) - \alpha_{\text{cross}}^{\mathcal{T}_{\text{eff}}}(0)| < \xi'$, which together indeed implies that O_{jj} is within distance $\delta' > 0$ of T_{jj} .

In order to show that the absolute value of the remaining off-diagonal elements of \mathcal{O}_{eff} must be close to zero (i.e., close to those of \mathcal{T}_{eff}) we consider the quantum states given by

$$|\mu_\theta(\alpha)\rangle = \frac{\sqrt{1 - \alpha}}{\sqrt{2}} (|0\rangle + |i\rangle) + e^{i\theta} \sqrt{\alpha} |j\rangle, \quad \text{with } \alpha \in [0, 1] \text{ and } \theta \in [0, 2\pi). \quad (29)$$

Its expectation value with respect to \mathcal{O}_{eff} is given by

$$\langle \mu_\theta(\alpha) | \mathcal{O}_{\text{eff}} | \mu_\theta(\alpha) \rangle = (1 - \alpha) \cdot (O_{00} + O_{ii} + \text{Re}(O_{0i})) + \alpha \cdot O_{jj} + \sqrt{2\alpha(1 - \alpha)} \cdot C_\theta, \quad (30)$$

where $C_\theta := \text{Re}(e^{i\theta}(O_{0j} + O_{ij}))$, and its expectation value with respect to \mathcal{T}_{eff} is given by

$$\langle \mu_\theta(\alpha) | \mathcal{T}_{\text{eff}} | \mu_\theta(\alpha) \rangle = (1 - \alpha) \cdot (T_{00} + T_{ii}) + \alpha \cdot T_{jj}. \quad (31)$$

Crucially, by our choice of \mathcal{T} we know that the label of $|\mu_\theta(\alpha)\rangle$ goes from -1 to $+1$ as α goes $0 \rightarrow 1$. Note that the expectation value of $|\mu_\theta(\alpha)\rangle$ with respect to \mathcal{T}_{eff} is independent from the phase θ .

To determine that $|O_{ij}|$ is smaller than $\delta'' > 0$ for $i, j \geq 1$ and $i \neq j$, we query the classifier $c_{\mathcal{O},b}$ on the states $|\gamma_{\hat{\theta}}(\hat{\alpha})\rangle$ for all $\hat{\theta}$ in a ζ'' -mesh of $[0, 2\pi)$ and for all $\hat{\alpha}$ in a ξ'' -mesh of $[0, 1]$ and we suppose they are labeled the same as the target classifier $c_{\mathcal{T},-1}$ would. Using these queries we can find estimates $\hat{\alpha}_{\text{cross}}^{\mathcal{O}_{\text{eff}}}(\hat{\theta})$ that are ξ -close to the unique $\alpha_{\text{cross}}^{\mathcal{O}_{\text{eff}}}(\theta) = \alpha'$ that satisfies

$$\langle \mu_\theta(\alpha') | \mathcal{O}_{\text{eff}} | \mu_\theta(\alpha') \rangle = 0, \quad (32)$$

by finding the smallest $\hat{\alpha}$ where the label has gone from -1 to $+1$. Because the label assigned by $c_{\mathcal{T},-1}$ does not depend on the phase θ , and since all states $|\mu_{\hat{\theta}}(\hat{\alpha})\rangle$ were assigned the same label by $c_{\mathcal{O},b}$ and $c_{\mathcal{T},-1}$, we find that the crossing point estimate $\hat{\alpha}_{\text{cross}}^{\mathcal{O}_{\text{eff}}}(\hat{\theta})$ is the same for all $\hat{\theta}$. In particular, this implies that the actual crossing points $\alpha_{\text{cross}}^{\mathcal{O}_{\text{eff}}}(\hat{\theta})$ have to be within ξ'' -distance of each other for all $\hat{\theta}$. Subsequently, write $O_{0j} + O_{ij} = |O_{0j} + O_{ij}|e^{i\phi}$ with $\phi \in [0, 2\pi)$, let $\hat{\theta}_{\text{abs}}$ denote the point in the ζ'' -mesh of $[0, 2\pi)$ that is closest to $2\pi - \phi$, and let $\hat{\theta}_0$ denote the point in the ζ'' -mesh of $[0, 2\pi)$ that is closest to $\pi/2 - \phi$ modulo 2π . By our previous discussion we know that $|\alpha_{\text{cross}}^{\mathcal{O}_{\text{eff}}}(\hat{\theta}_{\text{abs}}) - \alpha_{\text{cross}}^{\mathcal{O}_{\text{eff}}}(\hat{\theta}_0)| < \xi''$, which implies

$$|C_{\hat{\theta}_{\text{abs}}} - C_{\hat{\theta}_0}| < h(\xi''), \quad (33)$$

where h is a continuous function (independent from $c_{\mathcal{O},b}$ and $c_{\mathcal{T},-1}$) with $h(\xi'') \rightarrow 0$ as $\xi'' \rightarrow 0$. Moreover, using the inequality $\cos(\zeta'') \geq 1 - \lambda\zeta''$, where $\lambda \approx 0.7246$ is a solution of $\lambda(\pi - \arcsin(\lambda)) = 1 + \sqrt{1 - \lambda^2}$, together with the inequality $\cos(\pi/2 - \zeta'') \leq \zeta''$, we can derive that

$$\begin{aligned} |C_{\hat{\theta}_{\text{abs}}} - C_{\hat{\theta}_0}| &= \left| |O_{0j} + O_{ij}| \cos(\hat{\theta}_{\text{abs}} + \phi) - |O_{0j} + O_{ij}| \cos(\hat{\theta}_0 + \phi) \right| \\ &\geq |O_{0j} + O_{ij}| \cdot |\cos(\zeta'') - \cos(\pi/2 - \zeta'')| \\ &\geq |O_{0j} + O_{ij}| \cdot |1 - (\lambda + 1)\zeta''|. \end{aligned} \quad (34)$$

Finally, by combining Equation (33) with Equation (34) we can conclude that

$$|O_{0j} + O_{ij}| < \frac{h(\xi'')}{1 - (\lambda + 1)\zeta''},$$

which for ξ'' and ζ'' small enough shows that $|O_{0j} + O_{ij}| < \delta''/2$ (i.e., the fineness of both meshes ξ'' and ζ'' will depend on the choice of δ''). In conclusion, to determine that $|O_{ij}|$ is smaller than $\delta'' > 0$ we first do the required queries to determine that $|O_{0j}| < \delta''/2$, after which we do the required queries to determine that $|O_{0j} + O_{ij}| < \delta''/2$, which together indeed implies that $|O_{ij}| < \delta''$.

All in all, we have described a (finite) set of states such that if the label assigned by $c_{\mathcal{O},b}$ agrees with the label assigned by $c_{\mathcal{T},-1}$, then the absolute value of the off-diagonal elements of the first row of \mathcal{O}_{eff} have to be smaller than δ , the diagonal elements of \mathcal{O}_{eff} have to be within δ' -distance of those of \mathcal{T}_{eff} , and the remaining off diagonal elements of \mathcal{O}_{eff} have to be smaller than δ'' . Finally, we choose $\delta, \delta', \delta'' = 1/2^{n+1}$ and use the above protocol to establish that for $1 \leq i \leq r-1$ the Gershgorin discs D_i of \mathcal{O}_{eff} (i.e., with center O_{ii} and radius $\sum_j |O_{ij}|$) have to be contained in the disks \tilde{D}_i with center $i+1$ and radius $1/2$. Moreover, we establish that the Gershgorin disc D_0 has

to be contained in the disks \tilde{D}_0 with center $-r + 1$ and radius $1/2$. Since the disks \tilde{D}_i are disjoint, so are the Gershgorin discs D_i , which implies that \mathcal{O}_{eff} must have at least r distinct eigenvalues, and thus that $\text{rank}(\mathcal{O}) \geq r$. Consequently, if $\text{rank}(\mathcal{O}) < r$, then $c_{\mathcal{O},b}$ must disagree with $c_{\mathcal{T},-1}$ on the label of at least one of the states queried during the protocol. \square

B.2 Proof of Proposition 6

Proposition 6. *Let $\mathcal{C}_{\text{lin}}(\Phi)$ denote the family of linear classifiers that is equipped with a feature map Φ . Also, let $\mathcal{C}_{\text{qlin}}^{(\leq r)}(\Phi')$ denote the family of quantum linear classifiers that uses observables of rank at most r and which is equipped with a quantum feature map Φ' . Then, the following statements hold:*

- (i) *For every feature map $\Phi : \mathbb{R}^\ell \rightarrow \mathbb{R}^N$ with $\sup_{x \in \mathbb{R}^\ell} \|\Phi(x)\| = M < \infty$, there exists a feature map $\Phi' : \mathbb{R}^\ell \rightarrow \mathbb{R}^{N+1}$ such that $\|\Phi'(x)\| = 1$ for all $x \in \mathbb{R}^\ell$ and the families of linear classifiers satisfy $\mathcal{C}_{\text{lin}}(\Phi) \subseteq \mathcal{C}_{\text{lin}}(\Phi')$.*
- (ii) *For every feature map $\Phi : \mathbb{R}^\ell \rightarrow \mathbb{R}^N$ with $\|\Phi(x)\| = 1$ for all $x \in \mathbb{R}^\ell$, there exists a quantum feature map $\Phi' : \mathbb{R}^\ell \rightarrow \text{Herm}(\mathbb{C}^{2^n})$ that uses $n = \lceil \log N + 1 \rceil + 1$ qubits such that the families of linear classifiers satisfy $\mathcal{C}_{\text{lin}}(\Phi) \subseteq \mathcal{C}_{\text{qlin}}^{(\leq 1)}(\Phi')$.*
- (iii) *For every quantum feature map $\Phi : \mathbb{R}^\ell \rightarrow \text{Herm}(\mathbb{C}^{2^n})$, there exists a classical feature map $\Phi' : \mathbb{R}^\ell \rightarrow \mathbb{R}^{4^n}$ such that the families of linear classifiers satisfy $\mathcal{C}_{\text{qlin}}(\Phi) = \mathcal{C}_{\text{lin}}(\Phi')$.*

Proof. (i): First, we define the feature map $\Phi' : \mathbb{R}^\ell \rightarrow \mathbb{R}^{N+1}$ which maps

$$x \mapsto \frac{\Phi(x)}{M} + \sqrt{1 - \frac{\|\Phi(x)\|^2}{M^2}} e_{N+1},$$

where e_{N+1} denotes the $(N+1)$ -th standard basis vector. Note that this feature map indeed satisfies that $\|\Phi'(x)\| = 1$ for all $x \in \mathbb{R}^\ell$. Next, for any classifier $c_{w,b} \in \mathcal{C}_{\text{qlin}}(\Phi)$ we define $w' = w$ and $b' = b/M$ and we note that for any $x \in \mathbb{R}^\ell$ we have

$$c_{w',b'}(\Phi'(x)) = \text{sign}(\langle w', \Phi'(x) \rangle - b') = \text{sign}(M^{-1}[\langle w, \Phi(x) \rangle - b]) = \text{sign}(\langle w, \Phi(x) \rangle - b) = c_{w,b}(\Phi(x)).$$

(ii): First, we define the feature map $\tilde{\Phi} : \mathbb{R}^\ell \rightarrow \mathbb{R}^{N+1}$ which maps

$$x \mapsto \Phi(x) + e_{N+1},$$

where e_{N+1} denotes the $(N+1)$ -th standard basis vector. Next, for any classifier $c_{w,b} \in \mathcal{C}_{\text{lin}}(\Phi)$ we define $\tilde{w} = w - b e_{N+1}$ and we note that for all $x \in \mathbb{R}^\ell$ we have

$$c_{\tilde{w},0}(\tilde{\Phi}(x)) = \text{sign}(\langle \tilde{\Phi}(x), \tilde{w} \rangle) = \text{sign}(\langle \Phi(x), w \rangle - b) = c_{w,b}(\Phi(x)).$$

Therefore, it suffices to show that we can implement any linear classifier on \mathbb{R}^{N+1} with $b = 0$ as a quantum linear classifier on $n = \lceil \log N + 1 \rceil + 1$ qubits. To do so, we define the quantum feature map $\Phi' : \mathbb{R}^\ell \rightarrow \text{Herm}(\mathbb{C}^{2^n})$ which maps

$$x \rightarrow \rho_x = \left(\frac{|\Phi(x)\rangle + |0\rangle}{\sqrt{2}} \right) \left(\frac{\langle \Phi(x)| + \langle 0|}{\sqrt{2}} \right),$$

where $|0\rangle$ is a vector that does not lie in the support of Φ (note this vector exists since we have chosen n large enough). Finally, for any linear classifier $c_{w,0} \in \mathcal{C}_{\text{lin}}(\Phi)$ on \mathbb{R}^{N+1} we define $b' = \|w\|^2/2$ and $\mathcal{O} = |w'\rangle\langle w'|$, where $|w'\rangle = |w\rangle + \|w\| |0\rangle$ and we note that for all $x \in \mathbb{R}$ we have

$$\begin{aligned} c_{\mathcal{O},b'}(\Phi'(x)) &= \text{sign}(\text{Tr}[\mathcal{O}\rho_x] - b') \\ &= \text{sign}\left(\frac{1}{2}\left|\langle w | \Phi(x)\rangle + \|w\|\right|^2 - \frac{\|w\|^2}{2}\right) \\ &= \text{sign}(\langle w, \Phi(x)\rangle) = c_{w,0}(\Phi(x)). \end{aligned}$$

(iii): This follows directly from the fact that $\text{Herm}(\mathbb{C}^{2^n}) \simeq \mathbb{R}^{4^n}$. \square

B.3 Proof of Proposition 7

Proposition 7. *Let $\mathcal{C}_{\text{qlin}}^{(\eta)}$ denote the family of quantum linear classifiers corresponding to all n -qubit observables of Frobenius norm η , that is,*

$$\mathcal{C}_{\text{qlin}}^{(\eta)} = \left\{ c(\rho) = \text{sign}(\text{Tr}[\mathcal{O}\rho] - d) \mid \mathcal{O} \in \text{Herm}(\mathbb{C}^{2^n}) \text{ with } \|\mathcal{O}\|_F = \eta, d \in \mathbb{R} \right\}. \quad (20)$$

Then, for every $\eta \in \mathbb{R}_{>0}$ and $0 < m \leq 2^n$ there exists a set of m examples consisting of binary labeled n -qubit pure states that satisfies the following two conditions:

- (i) *There exists a classifier $c \in \mathcal{C}_{\text{qlin}}^{(\eta)}$ that correctly classifies all examples with margin η/\sqrt{m} .*
- (ii) *No classifier $c' \in \mathcal{C}_{\text{qlin}}^{(\eta')}$ with $\eta' < \eta$ can classify all examples correctly with margin $\leq \eta/\sqrt{m}$.*

Proof. Define $\mathcal{D}_m = \mathcal{D}_m^+ \cup \mathcal{D}_m^-$ whose positive examples (i.e., labeled $+1$) are given by

$$\mathcal{D}_m^+ = \left\{ |i\rangle\langle i| \mid i = 1, \dots, \frac{m}{2} \right\},$$

and whose negative examples (i.e., labeled -1) are given by

$$\mathcal{D}_m^- = \left\{ |i\rangle\langle i| \mid i = \frac{m}{2} + 1, \dots, m \right\}.$$

To classify this set of examples we take the classifier $c_{\mathcal{O},0} \in \mathcal{C}_{\text{qlin}}^{(\eta)}$ whose observable is given by

$$\mathcal{O} = \frac{\eta}{\sqrt{m}} \left(\left(\sum_{i=1}^{m/2} |i\rangle\langle i| \right) + \left(\sum_{j=\frac{m}{2}+1}^m |j\rangle\langle j| \right) \right).$$

We remark that $c_{\mathcal{O},0}$ can indeed classify the set of examples \mathcal{D}_r with margin η/\sqrt{m} .

Now suppose $c_{\mathcal{O}',b'} \in \mathcal{C}_{\text{qlin}}^{\eta'}$ with $\eta' < \eta$ can classify \mathcal{D}_m with margin γ' , that is

$$\text{Tr}[\mathcal{O}' |i\rangle\langle i|] \begin{cases} \geq b' + \gamma' & \text{if } i = 1, \dots, \frac{m}{2}, \\ \leq b' - \gamma' & \text{if } i = \frac{m}{2} + 1, \dots, m. \end{cases} \quad (35)$$

Define $\rho_+ = \sum_{i=1}^{m/2} |i\rangle\langle i|$ and $\rho_- = \sum_{i=\frac{m}{2}+1}^m |i\rangle\langle i|$ and note that Equation (35) implies that

$$\mathrm{Tr}[\mathcal{O}'\rho_+] \geq \frac{m}{2}b' + \frac{m}{2}\gamma'$$

and that

$$\mathrm{Tr}[\mathcal{O}'\rho_-] \leq \frac{m}{2}b' - \frac{m}{2}\gamma'$$

By combining these two inequalities we find that

$$\mathrm{Tr}[\mathcal{O}'(\rho_+ - \rho_-)] \geq \frac{m}{2}b' - \frac{m}{2}b' + \frac{m}{2}\gamma' + \frac{m}{2}\gamma' = m\gamma'. \quad (36)$$

Finally, by the Cauchy–Schwarz inequality we find that

$$\mathrm{Tr}[\mathcal{O}'(\rho_+ - \rho_-)] \leq \underbrace{\|\mathcal{O}'\|_F}_{<\eta} \cdot \underbrace{\|\rho_+ - \rho_-\|_F}_{=\sqrt{m}} < \eta\sqrt{m}. \quad (37)$$

Combining Equation (36) and (37) we find that

$$m\gamma' \leq \mathrm{Tr}[\mathcal{O}'(\rho_+ - \rho_-)] < \eta\sqrt{m}$$

from which we can conclude that $\gamma' < \eta/\sqrt{m}$.

□